Trace element composition of fluorite and its potential use as an indicator in mineral exploration

Mao Mao[1, a], George J. Simandl[1, 2], Jody Spence[2], Michaela Neetz[1], and Daniel Marshall[3]

[1] British Columbia Geological Survey, Ministry of Energy and Mines, Victoria, BC, V8W 9N3
[2] School of Earth and Ocean Sciences, University of Victoria, Victoria, BC, V8P 5C2
[3] Department of Earth Sciences, Simon Fraser University, Burnaby, BC, V5A 1S6
[a] corresponding author: Mao.Mao13@outlook.com

Recommended citation: Mao, M., Simandl, G.J., Spence, J., Neetz, M., and Marshall, D., 2016. Trace element composition of fluorite and its potential use as an indicator in mineral exploration. In: Geological Fieldwork, 2015, British Columbia Ministry of Energy and Mines, British Columbia Geological Survey Paper 2016-1, pp. 181-206.

Abstract

Fluorite is an accessory and a gangue mineral in many metalliferous deposits, and the trace element composition of fluorite has been used to discriminate different deposit types. We examined fluorite from 14 North American deposits by performing 514 LA-ICP-MS analyses for thirty-four elements, to improve our database. This database will be required for future studies aiming to produce reliable discrimination diagrams for use in mineral exploration. Results of this study revealed that fluorite from sedimentary-hosted deposits (Liard, Kootenay Florence, vein; Hastie Quarry, Barnett mine, Elmwood, Gordonsville, Young mine, MVT) has Sr concentrations less than 200 ppm (with the exception of two outliers), and Y concentrations less than 31 ppm. REE chondrite-normalized patterns are convex or have a negative slope; 75% of the data have a chondrite-normalized REE ratio below 3. Seventy-five percent of fluorite analyses from peralkaline/alkaline-related deposits (Kipawa, Rexspar, Eaglet, Rock Candy), and Rock Canyon Creek have chondrite-normalized ratios higher than 2 for each lanthanide, and flat to weakly negative patterns. The 4th tetrad portion of the chondrite-normalized REE plots of sedimentary-hosted deposits has a weakly negative to negative slope, whereas the pattern for alkaline/peralkaline-related deposits varies from weakly negative to positive. Fifty percent of the data (between the 1st and 3rd quartile) from carbonatite-related deposits (Eldor and Wicheeda Lake) show sinusoidal patterns on chondrite-normalized REE plots, with wide element ranges in their first tetrad. Barium, Th, and U also show potential for use in indicator mineral discrimination diagrams. Analyses of single crystals reveals compositional zoning that may not be optically apparent. Fifty analyses on a single Rock Candy fluorite crystal identified three compositional zones. One of these zones shows variations of trace elements (Ce, 14.5%; Pr, 13.9%; Nd, 14.9%; Sm, 16.9%; Eu 11.4%; Gd, 19.2%; Dy, 18.8%) with similar or lower variability than NIST glass (615). This zone may be useful as a matrix-matched secondary standard. Intra-grain chemical zoning is unlikely to be a major cause of elemental variation within a deposit and, by extrapolation, between deposit types. Our results suggest that Y, Sr and REE are essential for constructing discrimination diagrams that use fluorite as an indicator mineral.

Keywords: Fluorite, REE, indicator mineral, exploration, LA-ICP-MS

1. Introduction

Fluorite (CaF_2) belongs to the isometric crystal system, with a cubic, face-centred lattice. Fluorite commonly forms cubes or octahedrons, and less commonly dodecahedrons. Single crystal fluorite is transparent to translucent, and has vitreous luster. Although fluorite can be colourless, it occurs in a variety of colours, including purple, green, blue, yellow, and can exhibit colour zoning (Staebler et al., 2006). Fluorite from many localities is fluorescent (Verbeek, 2006).

Fluorite density varies from 3.0-3.6 g/cm^3, depending to a large extent on inclusions and impurities in the crystal lattice (Staebler et al., 2006). The Ca^{2+} ion in the fluorite crystal structure can be replaced by Li^+, Na^+, K^+, Mg^{2+}, Mn^{2+}, Fe^{2+}, Fe^{3+}, Zn^{2+}, Sr^{2+}, Y^{3+}, Zr^{4+}, Ba^{2+}, Pb^{2+}, Th^{4+}, U^{4+}, and lanthanide ions (Bailey et al., 1974; Bill and Calas, 1978; Gagnon et al., 2003; Schwinn and Markl, 2005; Xu et al., 2012; Deng et al., 2014). It is expected that the colour zoning observed in many fluorite crystals is manifested by corresponding variations in concentrations of trace elements. Sector zoning (e.g., [111] relative to [100] sector), reflecting preferential substitution and incorporation of trace elements was described by Bosze and Rakovan (2002). Concentrations of impurities in fluorite commonly do not exceed 1% (Deer et al., 1965).

Fluorite, as an accessory and a gangue mineral, occurs in many metalliferous deposits and, in exceptional cases, it can be the main ore of an economic deposit (Simandl, 2009). Fluorite commonly occurs adjacent to or in: carbonatites and alkaline complexes (Kogut et al., 1998; Hagni,1999; Alvin et al., 2004; Xu et al., 2004; Salvi and Williams-Jones, 2006); Mississippi Valley-type (MVT) Pb-Zn-F-Ba deposits; F-Ba-(Pb-Zn) veins (Grogan and Bradbury, 1967,1968; Baxter et al., 1973; Kesler et al., 1989; Cardellach et al., 2002; Levresse et al., 2006); hydrothermal Fe (±Au, ±Cu) and rare earth element (REE) deposits (Borrok et al., 1998; Andrade et al.,1999; Fourie, 2000); precious metal concentrations (Hill et al., 2000); skarns (Lu et al., 2003); Sn-polymetallic greissen-type deposits (Bettencourt et al., 2005); and uranium deposits (Cunningham et al., 1998; Min et al., 2005).

Based on its physical and chemical properties, and its association with diverse deposit types, fluorite can be used as

a proximal indicator mineral for mineralization if appropriate discrimination diagrams are established. The trace element distribution in fluorite of ore deposits has been previously studied by Möller et al. (1976), Bau et al. (2003), Gagnon et al. (2003), Schwinn and Markl (2005), and Deng et al. (2014). The benchmark paper by Möller et al. (1976) divided the Tb/Ca vs Tb/La diagram into sedimentary, hydrothermal, and pegmatitic fields. Eppinger and Closs (1990) investigated fluorite in south-central New Mexico, showing that Sr, Ba, Y, and U composition and Eu anomalies are useful in identifying fluorite from epithermal Au-Ag-Cu-Pb-Zn veins, W-Be-Fe skarns, epithermal Ba-Pb veins, and epithermal calcite-silica-fluorite veins. Gagnon et al. (2003) studied the Gallinas Mountains (New Mexico), Rock Canyon Creek (British Columbia), South Platte (Colorado), and St. Lawrence (Newfoundland) deposits. They concluded that chondrite-normalized REE patterns for fluorite from granite-related deposits and alkaline rock-related deposits are distinct. Schwinn and Markl (2005) investigated the REE behaviors of hydrothermal fluorite, showing that the REE are carried by basement-derived hydrothermal fluids, and not from the country rock adjacent to fluorite mineralization. More recently, Makin et al. (2014) compiled trace-element concentrations of fluorite from MVT, fluorite-barite veins, peralkaline-related, and carbonatite-related deposits to validate the previously published diagram by Möller et al. (1976).

A preliminary survey (Mao et al., 2015) investigated fluorite from the Rock Candy deposit (British Columbia), Kootenay Florence (British Columbia), Eaglet (British Columbia), Eldor (Quebec), and the Hastie quarry (Illinois) by laser ablation-inductively coupled mass spectrometry (LA-ICP-MS) analysis of individual grains and powder fused beads, and by X-ray fluorescence (XRF) analysis. Their results showed that Sr, Y, and lanthanides concentrations in fluorite can be reliably measured by LA-ICP-MS, and these elements have the potential to discriminate fluorite from different deposit types. Other elements, such as Mn, Ba, and Th are present in detectable levels in some deposits and may further contribute to discriminating deposit types. The same study confirmed that the stoichiometric Ca content of fluorite can be used as the internal standard for LA-ICP-MS analysis of fluorite.

A matrix-matched standard of fluorite for LA-ICP-MS analysis is currently unavailable because reference minerals with homogeneous trace element contents are scarce (Klemme et al., 2008). Previous LA-ICP-MS studies on trace elements in fluorite used National Institute of Standards and Technology (NIST) glasses as the main external standard and Ca as the internal standard (Gagnon et al., 2003; Schwinn and Markl 2005; Dimitrova et al., 2011; Baele et al., 2012). Jackson (2008) showed that fluorite REE contents analyzed by LA-ICP-MS using non-matrix-matched standards (10-100 ppm) agree well with results from solution nebulization-ICP–MS. However, Jackson (2008) and Sylvester (2008) also revealed that large errors can occur when the fractionation indices of elements differ substantially from those of the internal standard. Therefore, finding a matrix-matched secondary standard would improve the accuracy of LA-ICP-MS analyses.

For this study, we analyzed samples from 14 North American deposits by LA-ICP-MS (Fig. 1; Table 1). The main objectives were to: 1) examine trace element variations in crystals; 2) evaluate the element composition of fluorite on a deposit scale; 3) document variations in chemical composition of fluorite from different deposit types; and 4) assess fluorite from Rock Candy as a matrix-matched secondary standard for LA-ICP-MS.

2. Laboratory methods

2.1. Sample preparation

In total, 36 rock samples from 14 deposits in North America were selected for use in this study (Table 2). Twenty-eight samples were broken to select fluorite fragments of sizes 0.2-2.5 cm. These fluorite fragments were then crushed and examined under a binocular microscope to select only inclusion-free fluorite fragments (0.5 mm to 3 mm). Grains from each inclusion-free fluorite concentrate were mounted and polished on epoxy pucks for trace element analysis of individual grains by LA-ICP-MS (Table 2). Another nine rock samples were prepared as polished thin sections 200 μm thick. These polished thin sections were analyzed by LA-ICP-MS for trace element concentrations.

Two single fluorite crystals were covered by 57 LA-ICP-MS analyses to determine the trace element variations on the crystal scale. One of these, a dodecahedron green fluorite (~1 cm in diameter) from the Rock Candy deposit, named RC-08-8X (from sample RC-08-8), was split close to its {111} cleavage and mounted with the cleavage face upward (Fig. 2). This Rock Candy crystal was selected because of its centimetre size and

Fig. 1. Location of the 14 deposits examined in this study.

Table 1. Summary of the fluorite-bearing deposits sampled for this study.

Deposit name	Deposit-type	Local Geology	Additional information	Mineral assemblage
Rock Canyon Creek, BC	Carbonatite or peralkaline intrusion related (fl±REE)	Cambro-Ordovician to Devonian carbonate rocks (Leech, 1979) disseminated and veinlet fl and brt associated with REE mineralization occurs in dolomite (Pell, 1992; Samson et al., 2001).	fl bearing rocks have high F, REE, Ba, Nb, Mo, Zn, Pb, Mg, Ag by whole-rock geochemistry (Samson et al., 2001; Gagnon et al., 2003).	Main zone: fl, brt, dol, qz, synchysite, parasite, bastnäesite, py, cal, gorceixite, ilt, ap. Float zone: fl, qz, brt, ms, crl, prosopite, elpasolite, goyazite, gorceixite (Samson et al., 2001).
Eldor, QC	Carbonatite-hosted REE±Nb ±Ta ±fl ±ap	carbonatite complex (1.88-1.87 Ga, U-Pb); pcl and columbite in the middle stage carbonatite; REE minerals and fl in the late stage carbonatite (Gagnon et al., 2012).	fl as intergrowths with mnz,; may incorporate aggregates of anhedral bastnaesite and small veins of xtm (Gagnon et al., 2012).	mnz, bastnaesite, parasite, synchysite, xtm, fl, dol, qz, ms, Accesssory minerals are ap, py, sp, mag, Nb-bearing rt, nioboaeschynite, ferrocolumbite and ilm (Wright et al., 1998; Gagnon et al., 2012).
Wicheeda lake, BC	Carbonatite-related LREE±Nb	steeply dipping lens of carbonatite in metasedimentary rocks (Trofanenko et al., 2014).	trace fl (Trofanenko et al., 2014); relationship to REE mineralization uncertain	Bastnäesite(Ce), mnz(Ce), pcl, cal, bt, py, ab, ap, fl (Trofanenko et al., 2014).
Rock Candy, BC	fl-brt vein	fl veins hosted by Tertiary andesites (adjacent to Coryell syenite) consisting of ab, oligoclase, act, bt, mag. altered andesite adjacent to veins contains chl, ser, qz, cal, py, clay minerals (Pell, 1992).	breccia and composite veins with multiple generations of green and purple fl are exposed in a trench, containing fragments of severely altered country rock (Pell, 1992).	fl, brt, chalcedony, kln, py, qz, and cal (Pell, 1992; Mauthner and Melanson, 2006).
Eaglet, BC	Mo- and fl-bearing granite-syenite	granitic orthogneiss (375-335 Ma, U-Pb zircon; Mortensen et al., 1987) with dikes and pods of aplite, pegmatite, lamprophyre, and feldspar porphyry dikes, adjacent to contact with the Neoproterozoic biotite-garnet metapelite (Pell, 1992).	fl veinlets, veins, and pods; disseminated mol near the fl mineralization but not overlapping (Hora et al., 2008).	qz, mol, fl, carbonate minerals, clt, prismatic REE-bearing carbonates, gn, sp, py, gp, dck, aln, pcl (Pell, 1992; Hora et al., 2008).
Rexspar, BC	Volcanic hosted fl	Devonian-Mississippian trachytic rocks host one fl and five uranium zones (Preto, 1978).	fl zone is affected by a fine-grained, brecciated, tuffaceous trachyte with pervasive potassic alteration (McCammon, 1955; Preto, 1978; Pell, 1992).	fl associated with qz, brt, mol, clt, str, ccp, gn, and bastnaesite (Pell, 1992); fl from banded py-fl facies was analysed.
Kipawa, QC	Peralkaline-related REE±Zr	eudialyte, mosandrite, britholite-bearing syenite gneisses (Allan, 1992).		foliated leucocratic syenite with15-20% amphiboles, and 80-85% feldspar ± fl, vlasovite, gittensite, mosandrite, zircon, titanite?, fosterite?, baestnasite? (Saucier et al., 2013)

Table 1. Continued.

Deposit name	Deposit-type	Local Geology	Additional information	Mineral assemblage
Kootenay Florence, BC	Sedimentary-hosted Ag-Pb-Zn veins and replacements	veins and replacements along contact of limestone and overlaying schist; fl was recovered from a cave (Fyles, 1967).	sample selected for this study was a coarse, open space filling fl.	qz, ca, sp, ga, py, ± fl (Pell, 1992; Schofield, 1920).
Liard, BC	Carbonate-hosted fl±wth±brt (MVT)	irregular lenses, veins, breccia zones, and replacements in limestone or along limestone- mudstone contacts (Woodcock, 1972; Pell, 1992).	morphology of the mineralized zones, association with an unconformity and temperature of homogenization (T_h) suggest affinity with MVT deposits. T_h in cal, sp , brt = 62-240°C; salinity ~6.4-17.0 wt% NaCl equivalent (Changkakoti et al., 1987).	fl, wth, and brt ± barytocalcite; gangue qz and cal (Pell, 1992).
Barnett mine, IL	MVT (fl±wth±brt ±Pb±Zn)	mineralization follows a fault in a Mississippian interlayered greenish gray shale and sandstone unit (Baxter et al., 1967; Denny and Counts, 2009).	detailed geological descriptions unavailable.	
Hastie Quarry, IL	MVT (fl±wth±brt ±Pb±Zn)	bedded replacement zones in Mississippian oolitic or fossiliferous limestones underlying a sandstone unit (Pelch et al., 2015) age of mineralization is 272±17 Ma (fl, Sm-Nd; Chesley et al., 1994).	steeply dipping faults and fractures interpreted as feeders for mineralizing fluids (Pelch et al., 2015).	fl in hydrothermal stage II and III with sp, gn, qz, and ccp; gangue minerals brt, wth, and cal in stage IV (Richardson and Pinckney, 1984; Pelch et al., 2015).
Gordonsville, TN	MVT (sp±fl±cal±brt)	mineralization in collapse breccias in Lower Ordovician dolostone; deposits in dolomitized limestones (Misra and Lu, 1992).	massive, open space-filling, and disseminated sp T_h in cal, sp , brt = 100-150°C; salinity ~18-23 wt% NaCl equivalent (Misra and Lu, 1992).	sp, fl, cal, brt, and minor ± dol, gn, and py (Misra and Lu, 1992).
Elmwood, TN	MVT (sp±fl±cal±brt)	same as Gordonsville	same as Gordonsville	same as Gordonsville
Young mine, TN	MVT (sp±fl±cal±brt)	dolostone and limestone	detailed geological descriptions unavailable.	

Mineral abbreviations according to Whitney and Evans (2010): ab (albite), aln (allanite), ap (apatite), brt (barite), bt (biotite), cal (calcite), ccp(chalcopyrite), chl (chlorite), clt (celestite), crl (cryolite), dck (dickite), dol (dolomite), fl (fluorite), gp (gypsum), gn (galena), ilm (ilmenite), ilt (illite), kln (kaolinite), mag (magnetite), mol (molybdenite), ms (muscovite), pcl (pyrochlore), py (pyrite), qz (quartz), rt (rutile), ser (sericite) sp (sphalerite), str (strontianite), wth (witherite), xtm (xenotime).

Table 2. Statistical summary of fluorite samples and analyses.

Deposit name/Location	Sample Name	Fluorite Colour	No. of Analyses LA-ICP-MS	Total analysis
Rock Canyon Creek, BC	RC-9A-1	Purple	8	
	RC-9A-2	Colourless/purple	11	
	RC-9C	Purple	12	
	DP-08-1	Purple	8	
	DP-08-2A	Purple	10	49
Eldor, QC	ELDOR2	Colourless/purple	23	
	ELDOR3	Colourless/purple	9	
	ELDOR4	Colourless/purple	8	40
Wicheeda lake, BC	WI	Purple	7	7
Rock Candy, BC	RC-08-1	Green	10	
	RC-08-5	Purple/Green	26	
	RC-08-7	Pale	12	
	RC-08-8	Green	13	
	RC-08-8X	Green	50	111
Eaglet, BC	EAGLET7	Purple	17	
	EAGLET9	Colourless	12	
	EAGLET11	Colourless/purple	9	38
Rexspar, BC	08-GS-FL	Purple	18	
	08-GS-61A	Colourless	13	31
Kipawa, QC	Kipawa1	Colourless/purple	22	22
Kootenay Florence, BC	AHS-1	Colourless	13	13
Liard, BC	Liard-1	Colourless/purple	24	
	Liard-2	Colourless/purple	9	33
Hastie Quarry, IL	HQ-12S-9E	Yellow/purple	24	
	HQ-12S-9EB	Yellow/purple	4	28
Barnett mine, IL	BM-28-12S-8EV(W)	Colourless	20	
	BM-28-12S-8EMV(P)	Purple	24	44
Gordonsville, TN	204-4	Colourless/purple	12	
	205-4	Colourless/blue	6	
	293-4	Colourless/blue	12	
	58-15	Colourless/blue	6	
	58#11	Colourless/blue	12	48
Elmwood, TN	20-78#8	Colourless/blue	13	13
Young mine, TN (Mascot-Jefferson city)	YM9215-01	Colourless/purple	4	
	YM9215-02	Colourless/purple	10	
	YM9215L-01	Colourless/purple	8	
	YM9215L-02	Colourless/purple	8	
	YM9215-1X	Colourless/purple	7	37
				514

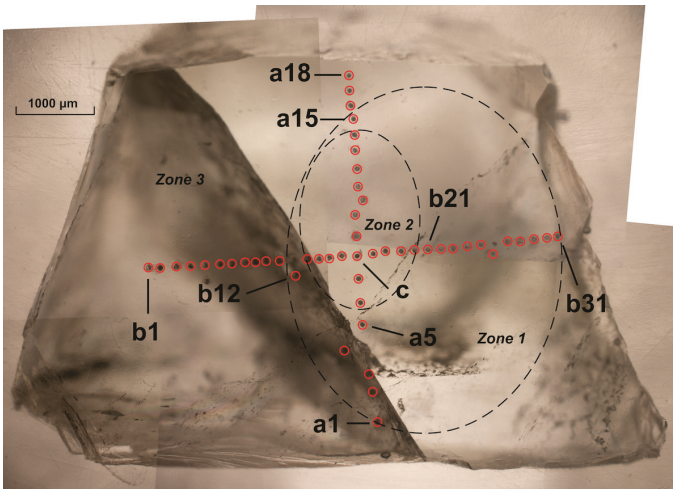

Fig. 2. Composite photo of sample RC-08-8X (Rock Candy Mine) in epoxy puck under plane-polarized light. The red circles indicate the location of LA-ICP-MS analyses along lines systematically numbered from 'a1-a18' (bottom to top) and 'b1-b31' (left to right) intersecting at point 'c'. Three analytical points (a4, b12, and b26) are offset from the lines 'a1-a18' and 'b1-b31'; to avoid impurities, original analyses on the line were discarded due to abnormal signals. Compositional zones delineated by dashed lines.

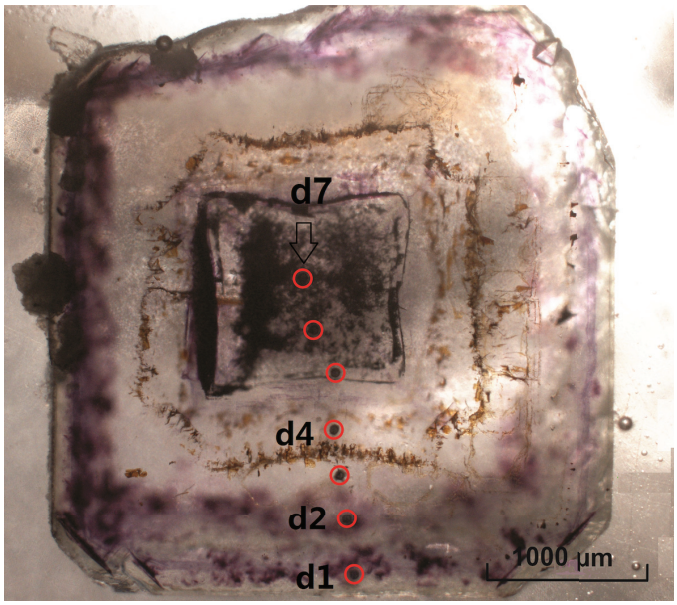

Fig. 3. Photo of the sample YM9215-1X in epoxy puck. The red circles indicate analytical points systematically numbered from 'd1-d7' (bottom to top).

lack of visible zoning using a petrographic microscope. The second sample is a cubic fluorite crystal with macroscopically visible colour zoning from Young mine, named YM9215-1X (derived from sample YM9215-01), which was mounted with the (001) face upward (Fig. 3).

2.2. LA-ICP-MS analysis

LA-ICP-MS analyses of fluorite grains were performed on a Thermo X-Series II (X7) quadrupole ICP-MS at the School of Earth and Ocean Sciences, University of Victoria. A New Wave UP-213 was coupled to the X-Series II with Helium as the carrier gas.

Fluorite grains were analyzed with a 55 µm diameter laser spot, a pulse rate of 10 Hz, and a measured fluence ranged from 7.69 to 12.55 J/cm^2. A pre-ablation warm-up of 5 seconds was used to avoid unstable laser energy at the beginning of each ablation. All spectra were recorded for 120 seconds including ~30 seconds gas blank before ablation started, 60 seconds during ablation, and ~30 seconds after ablation. At least 60 seconds of gas flushing occurred between analyses. The ICP-MS was optimized to maximize sensitivity and minimize oxide formation. Forward radio frequency ablation was carried out at 1400 watts. The dwell time was 10 ms for all elements.

The stoichiometric Ca content (51.33 wt.%) of fluorite was used as the internal standard for LA-ICP-MS calibration (Mao et al., 2015), whereas NIST glass standards (611, 613, 615) were used for external calibration (Jochum et al., 2011). Each analysis session started with NIST glasses 615, 613, and 611, followed by sample RC-08-8X, and then six to seven unknowns, before all four standards were repeated. During data reduction, time-resolved count rates were carefully checked and any spectra with spikes, indicating possible inclusions, were excluded. The data reduction procedure for each element was as follows: 1) selection of the time intervals for the background and signal region of each spectrum; 2) calculation of the mean CPS (counts per second) of these intervals; 3) background correction of the signal CPS; 4) external and internal standard normalizations; 5) drift correction using a linear drifting factor determined from repeat analysis of NIST 611; and 6) calibration using sensitivities for each element determined from the initial analyses of NIST 615, 613 and 611 in each load.

Thirty-four trace elements were analyzed by LA-ICP-MS for reconnaissance. The experimental precision was determined by repeat analyses of NIST glasses 613 and 615. Based on NIST 613, the 2σ precision for elements with concentrations ranging from tens to several hundred ppm is <5% for Mn, Sr, and Nb; from 5% to 10% for Mg, Sc, Ti, V, Cu, Zn, Rb, Y, Zr, Mo, Ba, lanthanides, W, Pb, and Th; and from 10% to 20% for Fe and U. For NIST 615, which contains lower concentrations of all elements than NIST 613, the 2σ precision is <15% for Mg, Pr, Eu, Tb, Ho, Tm, Lu, Pb, and Th; between 15-20% for Rb, Sr, Y, Zr, Nb, Ba, La, Nd, Sm, Dy, Er, Yb, and W; from 20% to 30% for V, Ce, Gd, and U; and >30% for other elements.

The limit of detection (LOD) was determined for each element using the following:

$$\mathrm{LOD} = \frac{3 \times (\mathrm{STDev\ background\ signal})}{\mathrm{Sensitivity(per\ analyte\ element,\ per\ session)}}$$

Where 'STDev background signal' is the standard deviation of the signal for a given element collected before ablation for each sample (gas blank), and 'Sensitivity' is the calibrated sensitivity determined from NIST 615, 613 and 611 in each session. Sensitivity = (corrected signal / element concentration).

The lower limits of detection are typically <20 ppm for Fe;

<15 ppm for Sr; <5 ppm for Mg; <3 ppm for Mn and Y; <2 ppm for Ba; <1 for Rb, Ce, Nd, and Pb; <0.5 for La, Pr, Sm, Gd, Dy, Th, and U; <0.2 for Zr, Nb, Mo, Eu, Tb, Ho, Er, Tm, Yb, Lu, and W.

3. Results

A total of 514 analyses were obtained from 38 samples (Table 2). The number of analyses per sample varied from 4 to 26, and many individual grains in these samples were analyzed twice to estimate trace element variations. At least 80% of the analyses have detectable levels of Sr, Y, and all lanthanides except Tm and Lu, which were detected in approximately 70% of analyses. In a few analyses, Mg, Mn, Zr, Ba, W, Th, and U are in concentrations above the detection limits. Iron is detectable in almost all analyses, but shows little variation in concentration. Few of the remaining elements are above their detection limits (Sc, V, Cu, Zn, Rb) or show little variations (Na, Ti, Nb, Mo, Pb) and hence will not be discussed further because they show limited potential for establishing discrimination diagrams.

3.1. Analytical results of trace elements by deposit (±2σ)

Strontium concentrations in analyzed fluorite grains vary from 3.41 (±0.57) to 3,530 (±180) ppm (Table 3; Fig. 4a). Fluorite from Eaglet has the highest Sr contents (1,830 ±90 – 3,530 ±180 ppm), followed by fluorite from Rexspar (1,110 ±60 – 1,640 ±80 ppm), Eldor (886 ±45 – 3,360 ±170 ppm), and Kipawa (952 ±48 – 1,240 ±60 ppm). Fluorite from Kootenay Florence, Liard, Hastie Quarry, Barnett mine, Young mine, Elmwood, Gordonsville, and Wicheeda Lake have Sr concentrations less than 200 ppm. Fluorite from the Elmwood has the lowest Sr contents (5.07 ±0.85 – 21.0 ±3.5 ppm), and the Gordonsville fluorite has the second lowest Sr contents (3.41 ±0.57 – 38.6 ±6.4 ppm). The range of Sr concentrations (3.41 ±0.57 – 808 ±40 ppm) in the Rock Canyon Creek samples overlap with the other deposits except for Eaglet, Rexspar, Eldor, and Kipawa. Fluorite from Rock Candy has a variation in Sr content from 125 (±6) to 701 (±35) ppm (Table 3; Figure 4a).

The term 'REE', as used in this paper, includes all lanthanides and Y (Sc will not be discussed due to its low concentrations in fluorite). The light REE (LREE) analyses include La, Ce, Pr, Nd, Sm, and Eu, and the heavy REE (HREE) analyses include Gd, Tb, Dy, Ho, Er, Tm, Yb, and Lu (Y is not included). From La to Eu, the general trends of element concentrations for all deposits do not show significant variations, and are summarized by the results of Ce (Fig. 4b). The deposits with consistently high Ce contents (Table 3; Fig. 4b) are Kipawa (15.1 ±0.8 – 120 ±7 ppm), and Rexspar (18.2 ±1.0 – 70.2 ±3.9 ppm). The Ce contents of fluorite from Rock Canyon Creek (0.01 ±0.003 – 205 ±11.2 ppm), Rock Candy (2.07 ±0.55 – 123 ±7 ppm), and Eldor (0.01 ±0.003 – 54.4 ±3.0 ppm) all show wide variations. Fluorite from Wicheeda Lake, Young mine, Kootenay Florence, Liard, Elmwood, Gordonsville, Barnett mine, and Hastie Quarry mostly have Ce contents less than 2 ppm (Fig. 4b). The lowest Ce contents are in Hastie Quarry fluorite (0.005 ±0.001 – 0.04 ±0.01 ppm), followed by Barnett mine (0.007 ±0.002 – 0.38 ±0.01 ppm). Neodymium shows similar concentration trends to Ce in all the deposits (Figs. 4b, c).

The element concentrations of HREE are summarized by the results of Gd (Fig. 4d). The highest contents of Gd are most commonly from Rexspar (5.95 ±0.42 – 32.4 ±2.3 ppm), followed by Kipawa (4.63 ±0.50 – 12.9 ±0.9 ppm), and are only surpassed by outliers of Eldor and values above the 3rd quartile from Rock Canyon Creek and Rock Candy. Fluorite from Rock Canyon Creek (0.76 ±0.16 – 45.4 ±3.2 ppm) and Rock Candy (0.06 ±0.01 – 109 ±7.7 ppm) show wide variations in Gd. The Young mine fluorite has the lowest Gd concentrations (0.01 ±0.002 – 0.27 ±0.05 ppm). Ytterbium shows similar concentration trends to Gd in all the deposits (Figs. 4d, e).

Yttrium ranges from 0.03 (±0.006) to 1,450 (±120) ppm (Table 3; Fig. 4f), with wide variations in samples from Rock Candy (0.50 ±0.09 – 1,450 ±120 ppm) and Rock Canyon Creek (1.15 ±0.22 – 946 ±77 ppm), which overlap with all other deposits except Young mine, which has the lowest Y concentrations (0.03 ±0.006 – 4.2 ±0.8 ppm, mostly <1 ppm). Besides Y in fluorite from Rock Candy and Rock Canyon Creek, there are very high Y contents in fluorite from Kipawa (132 ±11 – 304 ±25 ppm), Rexspar (92.8 ±7.5 – 645 ±52 ppm), and Eldor (104 ±8 – 866 ±70 ppm). Fluorite from Kootenay Florence, Liard, Hastie Quarry, Barnett mine, Young mine, Elmwood, Gordonsville, and Wicheeda Lake have less than 31 ppm Y. The Y concentrations in Eaglet samples vary from 27.7 (±2.2) to 74.1 (±6.0) ppm (Table 3; Fig. 4f).

The behaviours of Ce and Eu can differ to those of the adjacent REEs due to their redox sensitivity. Large variations in Ce anomalies

$$(Ce/Ce^{*} = \frac{(Ce/Ce_{ch})}{\sqrt{[(La/La_{ch}) x (Pr/Pr_{ch})]}}$$; Taylor and McLennan, 1985)

are seen in Hastie Quarry (0.43-1.25), Barnett mine (0.5-1.12), Rock Candy (0.69-1.05), and Eldor (0.6-1.06; Fig. 5a) samples. Sixty percent of the Ce anomalies from Eaglet are positive (>1). Fluorite from Young mine, Elmwood and Kipawa have Ce anomalies less than 0.93. Fluorite from Kootenay Florence (0.48-0.64) and Liard (0.51-0.68) have the strongest negative (<1) Ce anomalies.

The Eu anomalies

$$(Eu/Eu^{*} = \frac{(Eu/Eu_{ch})}{\sqrt{[(Sm/Sm_{ch}) x (Gd/Gd_{ch})]}}$$; Taylor and McLennan, 1985)

of fluorite range from 0.17 to 4.1, but most are between 0.2 and 2.8 (Fig. 5b). Fluorite from the Barnett mine shows the widest range in Eu anomalies, which are all positive (1.07-4.0). Generally, fluorite from Eldor and Rock Canyon Creek has very small Eu anomalies (Eu/Eu* = 0.8–1.3, median = 1.05). Most of the fluorite from Rock Candy, Elmwood, and Gordonsville has weak, positive Eu anomalies with magnitudes from 0.82 to 2.2. The remaining deposits generally have negative Eu anomalies. Kipawa has consistently strong negative Eu anomalies (Eu/Eu* = 0.32–0.37).

The main discriminations for lanthanides and Y in fluorite from the different deposits are listed below.

Table 3. Summary of trace-element contents (ppm) in fluorite grains. M.D.L.: Minimum Detection Limit. For each element, results below detection limit have been replaced with half the minimum detection limit from all analysis sections.

		Rock Canyon Creek			n=49		**Eldor**			n=40	**M.D.L.**
(ppm)	Minimum	1st quartile	Median	3rd quartile	Maximum	Minimum	1st quartile	Median	3rd quartile	Maximum	
Na	1.200	61.000	188.000	467.000	1730.000	1.200	1.200	13.200	17.400	64.100	2.402
Mg	0.470	0.470	22.500	97.400	582.000	0.470	0.470	0.470	2.780	23.200	0.942
Sc	0.130	0.130	0.130	1.120	11.100	0.130	0.130	0.130	0.130	0.130	0.267
Ti	0.060	0.410	0.510	0.510	5.070	0.020	0.070	0.510	0.510	0.510	1.021
V	0.020	0.040	0.040	0.040	0.470	0.040	0.040	0.040	0.040	3.390	0.082
Mn	0.360	0.360	0.360	2.210	39.000	0.360	0.360	0.360	0.360	0.360	0.717
Fe	129.000	154.000	171.000	234.000	281.000	104.000	119.000	134.000	166.000	219.000	2.800
Cu	0.120	0.160	0.160	0.160	8.290	0.160	0.160	0.160	0.160	9.260	0.317
Zn	0.040	0.040	0.040	0.040	0.120	0.040	0.040	0.040	0.040	2.810	0.074
Rb	0.020	0.030	0.030	0.030	8.070	0.030	0.030	0.030	0.030	0.030	0.059
Sr	3.410	59.200	212.000	357.000	808.000	886.000	982.000	1010.000	1120.000	3360.000	0.300
Y	1.150	9.310	70.400	118.000	946.000	104.000	152.000	167.000	197.000	866.000	0.065
Zr	0.002	0.030	0.030	1.470	11.300	0.002	0.003	0.010	0.030	0.040	0.004
Nb	0.003	0.020	0.020	1.010	6.230	0.001	0.003	0.020	0.020	0.050	0.003
Mo	0.010	0.080	0.110	0.340	0.740	0.004	0.010	0.070	0.110	0.110	0.215
Ba	0.010	0.010	1.890	11.500	83.700	0.010	0.010	0.020	0.560	2.200	0.027
La	0.010	0.740	8.380	27.600	124.000	0.010	0.110	0.280	0.940	56.800	0.027
Ce	0.010	2.440	16.400	41.600	205.000	0.010	0.440	0.720	1.910	54.400	0.023
Pr	0.010	0.600	1.820	4.450	15.800	0.010	0.110	0.150	0.330	4.920	0.016
Nd	0.050	4.490	6.740	18.300	76.000	0.050	0.860	1.070	1.810	18.400	0.091
Sm	0.240	1.480	2.400	4.750	15.600	0.050	0.680	0.770	0.910	5.790	0.105
Eu	0.120	0.560	0.840	2.270	6.850	0.010	0.460	0.490	0.560	3.590	0.029
Gd	0.760	1.720	2.730	7.160	45.400	1.460	2.300	2.430	2.790	18.200	0.110
Tb	0.110	0.230	0.350	1.040	4.260	0.010	0.460	0.490	0.550	4.460	0.014
Dy	0.460	1.570	2.600	9.390	41.400	2.380	3.550	3.940	4.430	39.200	0.083
Ho	0.060	0.250	0.580	1.560	11.200	0.010	0.790	0.890	0.990	8.220	0.020
Er	0.140	0.550	2.070	3.810	38.400	1.330	2.310	2.640	2.940	20.800	0.042
Tm	0.010	0.050	0.280	0.450	5.600	0.010	0.260	0.300	0.340	1.960	0.013
Yb	0.030	0.340	1.770	2.750	37.600	0.810	1.720	1.910	2.110	8.700	0.050
Lu	0.010	0.040	0.230	0.340	4.820	0.010	0.210	0.260	0.280	1.240	0.011
W	0.000	0.020	0.070	0.230	0.710	0.001	0.020	0.030	0.080	0.240	0.048
Pb	0.010	0.240	0.590	1.770	10.500	0.010	0.010	0.010	0.020	1.530	0.020
Th	0.420	2.490	7.770	53.500	108.000	0.003	0.010	0.010	0.030	0.260	0.012
U	0.001	0.005	0.020	0.080	3.220	<0.001	0.005	0.005	0.005	0.005	0.010

Table 3. Continued.

	Wicheeda lake				n=7	Eaglet				n=38	M.D.L.
(ppm)	Minimum	1st quartile	Median	3rd quartile	Maximum	Minimum	1st quartile	Median	3rd quartile	Maximum	
Na	1.200	1.200	1.200	39.000	75.400	1.200	1.200	15.000	19.200	40.000	2.402
Mg	0.470	0.470	0.470	0.470	82.000	0.470	0.470	0.470	0.470	3.290	0.942
Sc	0.130	0.130	0.130	0.130	0.130	0.030	0.130	0.130	0.130	0.130	0.267
Ti	0.030	0.390	0.510	0.510	0.510	0.030	0.090	0.510	0.510	0.510	1.021
V	0.040	0.040	0.040	0.040	0.040	0.040	0.040	0.040	0.040	0.040	0.082
Mn	0.360	0.360	0.360	0.360	32.100	0.360	3.940	4.770	5.490	7.960	0.717
Fe	193.000	222.000	234.000	246.000	258.000	120.000	139.000	151.000	169.000	201.000	2.800
Cu	0.120	0.150	0.160	0.160	0.170	0.110	0.160	0.160	0.160	0.160	0.317
Zn	0.040	0.040	0.040	0.040	0.080	0.040	0.040	0.040	0.040	1.790	0.074
Rb	0.030	0.030	0.030	0.080	0.230	0.030	0.030	0.030	0.030	0.030	0.059
Sr	12.400	14.400	37.000	53.900	60.200	1830.000	2350.000	2600.000	2810.000	3530.000	0.300
Y	3.540	4.540	6.080	10.800	17.500	27.700	30.200	49.300	55.000	74.100	0.065
Zr	0.030	0.030	0.030	0.030	0.030	0.002	0.010	0.030	0.030	0.030	0.004
Nb	0.002	0.003	0.020	0.050	0.070	0.001	0.010	0.020	0.020	0.230	0.003
Mo						0.010	0.070	0.110	0.190	0.520	0.215
Ba	0.010	0.630	3.560	5.440	5.840	0.010	0.010	0.010	0.020	0.080	0.027
La	0.010	0.010	0.010	0.180	3.060	0.830	1.480	2.530	3.250	5.090	0.027
Ce	0.010	0.010	0.010	0.190	2.040	2.660	5.400	7.890	8.890	11.700	0.023
Pr	0.010	0.010	0.010	0.010	0.280	0.010	0.910	1.180	1.330	2.440	0.016
Nd	0.050	0.050	0.050	0.070	1.000	4.430	5.120	5.640	6.340	14.400	0.091
Sm	0.020	0.020	0.050	0.050	0.310	0.950	1.140	1.360	2.250	4.180	0.105
Eu	0.010	0.010	0.010	0.020	0.080	0.010	0.330	0.370	0.710	1.610	0.029
Gd	0.050	0.050	0.060	0.300	0.390	1.350	1.580	1.880	3.440	5.170	0.110
Tb	0.010	0.020	0.030	0.040	0.060	0.010	0.220	0.250	0.400	0.650	0.014
Dy	0.100	0.120	0.240	0.260	0.280	1.310	1.510	1.720	2.600	3.550	0.083
Ho	0.020	0.030	0.050	0.060	0.070	0.010	0.350	0.410	0.550	0.680	0.020
Er	0.060	0.070	0.110	0.180	0.200	0.970	1.130	1.340	1.560	2.210	0.042
Tm	0.003	0.010	0.010	0.020	0.020	0.010	0.120	0.160	0.190	0.280	0.013
Yb	0.020	0.030	0.040	0.060	0.080	0.030	0.920	0.990	1.110	1.610	0.050
Lu	0.002	0.002	0.010	0.010	0.010	0.010	0.090	0.110	0.140	0.180	0.011
W	0.010	0.010	0.010	0.010	0.010	0.020	0.100	0.120	0.150	0.200	0.048
Pb	0.010	0.010	0.010	0.010	0.010	0.010	0.010	0.010	0.030	0.070	0.020
Th	0.010	0.010	0.330	4.310	22.700	0.001	0.003	0.010	0.010	11.000	0.012
U	0.003	0.004	0.005	0.080	0.270	0.003	0.005	0.010	0.020	0.150	0.010

Table 3. Continued.

			Kipawa		n=22			**Rexspar**		n=31	**M.D.L.**
(ppm)	Minimum	1st quartile	Median	3rd quartile	Maximum	Minimum	1st quartile	Median	3rd quartile	Maximum	
Na	1.200	45.900	64.700	86.500	168.000	1.200	58.100	77.100	122.000	683.000	2.402
Mg	0.470	0.470	0.470	0.470	4.110	0.470	0.470	0.470	3.810	10.100	0.942
Sc	0.130	0.130	0.130	0.130	0.130	0.130	0.130	0.130	0.130	0.130	0.267
Ti	0.020	0.120	0.510	0.510	2.200	0.040	0.070	0.180	0.510	0.510	1.021
V	0.010	0.040	0.040	0.040	0.040	0.040	0.040	0.040	0.040	0.040	0.082
Mn	0.360	0.360	0.360	1.220	1.920	2.920	4.360	4.980	5.470	7.510	0.717
Fe	122.000	136.000	148.000	152.000	170.000	109.000	124.000	138.000	176.000	199.000	2.800
Cu	0.160	0.160	0.160	0.160	0.160	0.160	0.160	0.160	0.160	0.160	0.317
Zn	0.040	0.040	0.040	0.040	0.040	0.040	0.040	0.040	0.040	1.810	0.074
Rb	0.030	0.030	0.030	0.030	0.030	0.030	0.030	0.030	0.030	0.190	0.059
Sr	952.000	1040.000	1090.000	1130.000	1240.000	1110.000	1280.000	1380.000	1430.000	1640.000	0.300
Y	132.000	162.000	203.000	269.000	304.000	92.800	112.000	151.000	194.000	645.000	0.065
Zr	0.001	0.010	0.010	0.030	0.030	0.002	0.030	0.030	0.030	0.610	0.004
Nb	0.001	0.010	0.020	0.020	0.060	0.003	0.020	0.020	0.020	0.040	0.003
Mo	0.010	0.010	0.020	0.040	0.110	0.020	0.090	0.110	0.110	0.190	0.215
Ba	0.540	0.620	0.700	0.930	1.390	0.010	0.010	0.010	0.270	3.400	0.027
La	7.320	11.400	20.900	31.900	49.500	8.150	13.300	17.300	23.500	29.200	0.027
Ce	15.100	25.100	41.700	62.800	120.000	18.200	31.800	39.100	56.800	70.200	0.023
Pr	2.610	4.050	5.820	8.730	14.500	2.710	4.950	5.660	8.350	11.800	0.016
Nd	14.200	19.600	28.000	42.300	56.700	14.900	25.200	29.000	42.700	71.900	0.091
Sm	3.490	4.680	6.860	9.300	11.000	4.570	6.040	7.850	10.200	22.700	0.105
Eu	0.500	0.590	0.880	1.150	1.350	1.550	2.060	2.540	3.560	7.410	0.029
Gd	4.630	6.370	8.750	10.800	12.900	5.950	8.010	9.330	12.700	32.400	0.110
Tb	0.690	0.920	1.220	1.650	1.910	0.720	0.930	1.160	1.480	3.960	0.014
Dy	4.900	6.640	8.670	11.700	13.300	4.300	5.540	6.810	8.430	23.300	0.083
Ho	1.120	1.570	2.020	2.580	3.050	0.870	1.080	1.360	1.730	4.840	0.020
Er	3.520	4.930	6.090	8.030	9.500	2.250	2.850	3.710	4.750	13.400	0.042
Tm	0.460	0.610	0.780	1.050	1.230	0.010	0.340	0.420	0.550	1.420	0.013
Yb	2.490	3.670	4.540	6.320	7.180	1.620	2.060	2.630	3.470	8.050	0.050
Lu	0.290	0.410	0.510	0.690	0.790	0.010	0.270	0.350	0.460	1.110	0.011
W	0.020	0.180	0.250	0.440	0.570	0.020	0.220	0.330	0.420	1.310	0.048
Pb	0.010	0.010	0.010	0.010	0.530	0.010	0.010	0.010	0.010	4.330	0.020
Th	0.010	0.010	0.010	0.010	12.800	0.010	0.010	0.020	0.070	0.200	0.012
U	0.005	0.005	0.030	0.080	0.100	0.005	0.005	0.090	0.130	0.240	0.010

Table 3. Continued.

	Rock Candy				n=60	RC-08-8X				n=51	M.D.L.
(ppm)	Minimum	1st quartile	Median	3rd quartile	Maximum	Minimum	1st quartile	Median	3rd quartile	Maximum	
Na	1.200	1.200	1.200	1.200	5.900	1.200	1.200	1.200	1.200	1.200	2.402
Mg	0.240	0.470	0.470	0.470	0.470	0.290	0.470	0.470	0.470	3.790	0.942
Sc	0.130	0.130	0.130	0.130	0.130	0.130	0.130	0.130	0.130	0.130	0.267
Ti	0.020	0.070	0.510	0.510	0.510	0.020	0.510	0.510	0.510	0.510	1.021
V	0.010	0.040	0.040	0.040	0.040	0.040	0.040	0.040	0.040	0.040	0.082
Mn	0.360	0.360	0.360	0.360	6.470	0.360	0.360	0.360	0.360	0.360	0.717
Fe	126.000	146.000	151.000	158.000	178.000	71.700	116.000	142.000	158.000	292.000	2.800
Cu	0.140	0.160	0.160	0.160	0.160	0.160	0.160	0.160	0.160	0.210	0.317
Zn	0.040	0.040	0.040	0.040	0.040	0.040	0.040	0.040	0.040	0.040	0.074
Rb	0.030	0.030	0.030	0.030	0.120	0.030	0.030	0.030	0.030	0.030	0.059
Sr	125.000	288.000	415.000	535.000	674.000	323.000	380.000	449.000	520.000	701.000	0.300
Y	0.500	5.030	16.800	35.300	1450.000	3.150	10.000	20.300	33.000	42.000	0.065
Zr	0.001	0.010	0.030	0.030	0.730	0.001	0.030	0.030	0.030	0.030	0.004
Nb	0.001	0.003	0.010	0.020	0.020	0.001	0.020	0.020	0.020	0.020	0.003
Mo	0.004	0.010	0.020	0.110	0.110	0.004	0.010	0.110	0.110	0.110	0.215
Ba	0.010	0.060	0.120	0.410	3.060	0.010	0.010	0.010	0.010	0.230	0.027
La	1.330	2.500	7.020	10.700	52.000	2.480	3.280	6.140	8.330	11.700	0.027
Ce	2.070	4.440	12.200	16.200	123.000	5.070	6.210	9.480	11.600	19.800	0.023
Pr	0.270	0.580	1.440	2.350	21.000	0.010	0.990	1.140	1.410	2.390	0.016
Nd	1.080	2.570	6.950	11.200	135.000	2.260	5.020	5.780	6.360	11.100	0.091
Sm	0.050	0.690	1.650	3.390	65.800	0.050	0.950	1.280	1.880	2.740	0.105
Eu	0.010	0.410	0.700	2.000	29.600	0.010	0.420	0.620	1.050	1.380	0.029
Gd	0.050	0.750	1.930	4.170	109.000	0.050	1.080	1.590	2.700	3.720	0.110
Tb	0.010	0.140	0.280	0.900	19.600	0.010	0.100	0.210	0.380	0.460	0.014
Dy	0.040	0.910	1.820	7.020	136.000	0.040	0.790	1.430	2.470	3.070	0.083
Ho	0.010	0.170	0.330	1.260	26.400	0.010	0.100	0.300	0.520	0.710	0.020
Er	0.020	0.510	0.900	3.830	67.800	0.020	0.410	0.920	1.550	2.060	0.042
Tm	0.000	0.070	0.140	0.570	6.930	0.010	0.010	0.120	0.190	0.250	0.013
Yb	0.030	0.500	1.040	4.050	36.000	0.030	0.510	0.850	1.330	1.790	0.050
Lu	0.010	0.070	0.160	0.510	3.980	0.010	0.010	0.130	0.210	0.290	0.011
W	0.001	0.003	0.020	0.020	0.270	0.001	0.020	0.020	0.020	0.020	0.048
Pb	0.003	0.010	0.010	0.010	0.100	0.010	0.010	0.010	0.010	0.010	0.020
Th	<0.001	0.010	0.010	0.040	0.970	0.010	0.010	0.010	0.010	0.070	0.012
U	0.002	0.005	0.010	0.030	3.170	0.005	0.005	0.005	0.090	0.430	0.010

Table 3. Continued.

	Kootenay Florence				n=13	Liard				n=33	M.D.L.
(ppm)	Minimum	1st quartile	Median	3rd quartile	Maximum	Minimum	1st quartile	Median	3rd quartile	Maximum	
Na	1.200	1.200	1.200	1.200	1.200	1.200	137.000	198.000	278.000	546.000	2.402
Mg	0.470	0.470	0.470	0.470	0.470	0.470	0.470	0.470	5.780	7.480	0.942
Sc	0.130	0.130	0.130	0.130	0.130	0.130	0.130	0.130	0.130	0.700	0.267
Ti	0.040	0.050	0.060	0.510	0.510	0.060	0.150	0.510	0.510	0.510	1.021
V	0.040	0.040	0.040	0.040	0.040	0.010	0.040	0.040	0.040	0.040	0.082
Mn	0.360	0.360	0.360	0.360	0.360	0.360	0.360	0.360	0.360	1.170	0.717
Fe	138.000	147.000	150.000	155.000	164.000	118.000	140.000	152.000	205.000	234.000	2.800
Cu	0.160	0.160	0.160	0.160	0.160	0.120	0.160	0.160	0.160	0.240	0.317
Zn	0.040	0.040	0.040	0.040	0.040	0.040	0.040	0.040	0.040	0.130	0.074
Rb	0.010	0.030	0.030	0.030	0.030	0.010	0.030	0.030	0.030	0.050	0.059
Sr	83.700	90.400	96.700	128.000	142.000	43.800	70.600	87.400	107.000	533.000	0.300
Y	6.040	13.500	16.000	20.600	31.500	6.140	20.400	22.300	23.800	28.700	0.065
Zr	0.003	0.004	0.030	0.030	0.030	0.004	0.360	0.540	0.670	0.890	0.004
Nb	0.020	0.020	0.020	0.020	0.020	0.002	0.010	0.020	0.020	0.020	0.003
Mo	0.010	0.080	0.110	0.110	0.110	0.010	0.010	0.090	0.110	0.110	0.215
Ba	0.010	0.010	0.010	0.040	0.510	0.010	3.200	15.400	31.500	474.000	0.027
La	0.010	0.430	0.780	0.970	1.130	0.010	0.160	0.220	0.280	0.370	0.027
Ce	0.010	0.480	0.780	1.100	1.370	0.010	0.320	0.370	0.410	0.490	0.023
Pr	0.010	0.040	0.160	0.210	0.230	0.010	0.010	0.080	0.100	0.120	0.016
Nd	0.050	0.780	0.940	1.220	1.600	0.050	0.360	0.560	0.670	0.810	0.091
Sm	0.050	0.130	0.300	0.370	0.590	0.030	0.050	0.200	0.250	0.280	0.105
Eu	0.010	0.010	0.080	0.110	0.220	0.010	0.010	0.070	0.090	0.110	0.029
Gd	0.050	0.340	0.760	0.880	1.080	0.050	0.600	0.720	0.840	3.460	0.110
Tb	0.010	0.010	0.070	0.110	0.150	0.010	0.050	0.100	0.110	0.140	0.014
Dy	0.040	0.420	0.630	0.760	1.080	0.040	0.600	0.730	0.800	1.040	0.083
Ho	0.010	0.010	0.100	0.160	0.240	0.010	0.140	0.170	0.180	0.210	0.020
Er	0.020	0.070	0.230	0.320	0.670	0.080	0.380	0.470	0.510	0.620	0.042
Tm	0.010	0.010	0.010	0.010	0.020	0.010	0.010	0.040	0.050	0.070	0.013
Yb	0.030	0.030	0.030	0.070	0.250	0.030	0.160	0.210	0.250	0.400	0.050
Lu	0.003	0.010	0.010	0.010	0.020	0.010	0.010	0.010	0.030	0.040	0.011
W	0.001	0.003	0.020	0.020	0.100	0.002	0.020	0.020	0.020	0.020	0.048
Pb	0.010	0.010	0.010	0.010	0.050	0.010	0.010	0.010	0.010	0.070	0.020
Th	0.010	0.010	0.120	0.240	0.290	0.010	0.100	0.190	0.270	0.810	0.012
U	<0.001	0.004	0.005	0.005	0.005	0.005	1.320	1.530	2.220	6.750	0.010

Table 3. Continued.

	Hastie quarry				n=28	Barnett Mine				n=44	M.D.L.
(ppm)	Minimum	1st quartile	Median	3rd quartile	Maximum	Minimum	1st quartile	Median	3rd quartile	Maximum	
Na	1.200	1.200	44.800	80.300	243.000	1.200	1.200	1.200	15.200	291.000	2.402
Mg	0.150	0.470	0.470	0.470	5.930	0.390	0.470	0.470	0.470	4.960	0.942
Sc	0.130	0.130	0.130	0.130	0.130	0.130	0.130	0.130	0.130	0.130	0.267
Ti	0.030	0.110	0.510	0.510	0.510	0.020	0.050	0.110	0.510	0.510	1.021
V	0.020	0.040	0.040	0.040	0.040	0.010	0.040	0.040	0.040	0.040	0.082
Mn	0.360	0.360	0.360	0.360	0.360	0.360	0.360	0.360	0.360	0.360	0.717
Fe	14.400	142.000	145.000	151.000	158.000	118.000	129.000	138.000	152.000	179.000	2.800
Cu	0.160	0.160	0.160	0.160	0.160	0.160	0.160	0.160	0.160	1.090	0.317
Zn	0.040	0.040	0.040	0.040	0.040	0.040	0.040	0.040	0.040	0.040	0.074
Rb	0.010	0.030	0.030	0.030	0.030	0.030	0.030	0.030	0.030	0.030	0.059
Sr	10.900	12.700	49.700	84.500	104.000	3.410	11.600	13.000	45.800	59.500	0.300
Y	2.620	3.050	9.970	12.200	13.100	0.970	2.110	2.670	6.140	8.220	0.065
Zr	0.002	0.002	0.010	0.030	0.030	0.001	0.010	0.030	0.030	0.030	0.004
Nb	0.001	0.001	0.020	0.020	0.020	0.001	0.002	0.020	0.020	0.030	0.003
Mo	0.005	0.010	0.110	0.110	0.110	0.003	0.010	0.020	0.110	0.110	0.215
Ba	0.002	0.010	0.040	0.140	0.170	0.001	0.010	0.010	0.010	0.550	0.027
La	0.001	0.003	0.010	0.010	0.010	0.001	0.010	0.010	0.040	0.100	0.027
Ce	0.005	0.010	0.010	0.040	0.040	0.010	0.010	0.020	0.150	0.380	0.023
Pr	0.001	0.010	0.010	0.020	0.020	0.002	0.010	0.010	0.050	0.090	0.016
Nd	0.040	0.050	0.150	0.260	0.290	0.050	0.050	0.080	0.370	0.550	0.091
Sm	0.050	0.050	0.150	0.240	0.270	0.050	0.050	0.050	0.130	0.280	0.105
Eu	0.010	0.010	0.070	0.100	0.120	0.010	0.050	0.080	0.230	0.330	0.029
Gd	0.050	0.170	0.500	0.660	0.740	0.050	0.110	0.160	0.350	0.620	0.110
Tb	0.010	0.010	0.070	0.090	0.100	0.010	0.010	0.020	0.030	0.050	0.014
Dy	0.040	0.120	0.450	0.560	0.610	0.040	0.100	0.140	0.230	0.360	0.083
Ho	0.010	0.010	0.090	0.110	0.120	0.010	0.010	0.020	0.040	0.080	0.020
Er	0.020	0.020	0.210	0.250	0.270	0.020	0.030	0.050	0.100	0.170	0.042
Tm	0.003	0.010	0.010	0.020	0.030	0.002	0.010	0.010	0.010	0.010	0.013
Yb	0.004	0.030	0.030	0.100	0.120	0.010	0.020	0.030	0.030	0.030	0.050
Lu	0.001	0.010	0.010	0.010	0.020	0.001	0.003	0.010	0.010	0.010	0.011
W	0.001	0.010	0.020	0.020	0.030	0.001	0.003	0.020	0.020	0.060	0.048
Pb	0.010	0.010	0.010	0.010	0.070	0.001	0.010	0.010	0.010	3.270	0.020
Th	0.010	0.010	0.180	0.300	0.380	0.010	0.010	0.010	0.020	0.040	0.012
U	0.001	0.005	0.005	0.010	0.010	<0.001	0.005	0.005	0.005	0.005	0.010

Table 3. Continued.

			Elmwood		n=13			**Gordonsville**		n=48	**M.D.L.**
(ppm)	Minimum	1st quartile	Median	3rd quartile	Maximum	Minimum	1st quartile	Median	3rd quartile	Maximum	
Na	1.200	1.200	1.200	1.200	17.400	1.200	1.200	1.200	8.240	149.000	2.402
Mg	0.470	0.470	0.470	0.470	0.470	0.310	0.470	0.470	0.470	25.000	0.942
Sc	0.130	0.130	0.130	0.130	0.130	0.130	0.130	0.130	0.130	0.130	0.267
Ti	0.510	0.510	0.510	0.510	0.510	0.510	0.510	0.510	0.510	0.510	1.021
V	0.040	0.040	0.040	0.040	0.040	0.010	0.040	0.040	0.040	0.040	0.082
Mn	0.360	0.360	0.360	0.360	0.360	0.360	0.360	0.360	0.360	0.360	0.717
Fe	74.500	79.400	89.200	101.000	108.000	89.200	106.000	121.000	129.000	150.000	2.800
Cu	0.160	0.160	0.160	0.160	0.160	0.160	0.160	0.160	0.160	0.830	0.317
Zn	0.040	0.040	0.040	0.040	0.040	0.040	0.040	0.040	0.040	53.100	0.074
Rb	0.030	0.030	0.030	0.030	0.030	0.010	0.030	0.030	0.030	0.030	0.059
Sr	5.070	6.710	10.700	15.800	21.000	3.410	8.490	10.600	14.300	38.600	0.300
Y	0.710	1.530	2.110	2.960	3.330	0.030	1.930	2.480	3.010	4.940	0.065
Zr	0.003	0.020	0.030	0.030	0.030	0.002	0.003	0.010	0.030	0.030	0.004
Nb	0.002	0.010	0.020	0.020	0.020	0.001	0.002	0.010	0.020	0.020	0.003
Mo	0.010	0.010	0.010	0.010	0.010	0.010	0.010	0.110	0.110	0.110	0.215
Ba	0.002	0.010	0.010	0.050	0.460	0.001	0.004	0.010	0.010	13.000	0.027
La	0.010	0.010	0.130	0.180	0.250	0.010	0.010	0.020	0.080	0.260	0.027
Ce	0.010	0.010	0.360	0.530	0.650	0.010	0.090	0.220	0.290	0.730	0.023
Pr	0.010	0.010	0.080	0.110	0.140	0.010	0.010	0.050	0.060	0.140	0.016
Nd	0.030	0.150	0.460	0.680	0.920	0.050	0.290	0.380	0.540	0.870	0.091
Sm	0.020	0.050	0.180	0.240	0.320	0.020	0.050	0.150	0.230	0.350	0.105
Eu	0.010	0.050	0.120	0.140	0.190	0.000	0.050	0.090	0.130	0.200	0.029
Gd	0.050	0.230	0.300	0.340	0.430	0.010	0.220	0.300	0.380	0.500	0.110
Tb	0.010	0.010	0.030	0.040	0.050	0.001	0.010	0.030	0.040	0.060	0.014
Dy	0.020	0.040	0.120	0.180	0.200	0.010	0.050	0.140	0.180	0.330	0.083
Ho	0.010	0.010	0.010	0.020	0.030	0.001	0.010	0.010	0.030	0.050	0.020
Er	0.020	0.020	0.020	0.050	0.080	0.003	0.020	0.020	0.050	0.090	0.042
Tm	0.002	0.003	0.004	0.010	0.010	<0.001	0.004	0.010	0.010	0.010	0.013
Yb	0.002	0.010	0.010	0.020	0.030	0.002	0.010	0.020	0.030	0.040	0.050
Lu	0.002	0.002	0.010	0.010	0.010	<0.001	0.002	0.004	0.010	0.010	0.011
W	0.003	0.003	0.020	0.020	0.020	0.001	0.001	0.004	0.020	0.020	0.048
Pb	0.001	0.005	0.010	0.010	0.010	0.001	0.010	0.010	0.010	0.810	0.020
Th	0.004	0.010	0.010	0.010	0.020	0.001	0.004	0.010	0.010	0.020	0.012
U	0.001	0.005	0.005	0.005	0.010	<0.001	0.001	0.005	0.005	0.005	0.010

Table 3. Continued.

			Young mine		n=30			**YM9215-1X**		n=7	**M.D.L.**
(ppm)	Minimum	1st quartile	Median	3rd quartile	Maximum	Minimum	1st quartile	Median	3rd quartile	Maximum	
Na	1.200	1.200	1.200	1.200	72.600	1.200	1.200	1.200	19.200	31.000	2.402
Mg	0.470	0.470	0.470	0.470	23.000	0.470	0.470	0.470	0.470	0.470	0.942
Sc	0.130	0.130	0.130	0.130	0.130	0.130	0.130	0.130	0.130	0.130	0.267
Ti	0.510	0.510	0.510	0.510	0.510	0.510	0.510	0.510	0.510	0.510	1.021
V	0.005	0.040	0.040	0.040	0.040	0.040	0.040	0.040	0.040	0.040	0.082
Mn	0.360	0.360	0.360	0.360	0.360	0.360	0.360	0.360	0.360	0.360	0.717
Fe	78.900	87.800	93.500	103.000	109.000	80.400	82.400	85.400	88.800	95.400	2.800
Cu	0.160	0.160	0.160	0.160	0.160	0.160	0.160	0.160	0.160	0.160	0.317
Zn	0.040	0.040	0.040	0.040	0.040	0.040	0.040	0.040	0.040	0.040	0.074
Rb	0.000	0.030	0.030	0.030	0.030	0.030	0.030	0.030	0.030	0.030	0.059
Sr	3.410	10.600	12.800	21.800	178.000	10.500	10.600	11.200	19.100	29.400	0.300
Y	0.030	0.030	0.090	0.210	4.200	0.030	0.030	0.030	0.080	0.240	0.065
Zr	0.002	0.003	0.030	0.030	0.140	0.002	0.002	0.002	0.002	0.002	0.004
Nb	0.001	0.002	0.003	0.020	0.020	0.001	0.001	0.001	0.010	0.020	0.003
Mo	0.005	0.005	0.010	0.110	0.110	0.110	0.110	0.110	0.110	0.110	0.215
Ba	0.002	0.010	0.010	0.010	0.260	0.004	0.004	0.010	0.010	0.010	0.027
La	0.010	0.710	1.160	1.700	12.900	0.010	0.460	1.140	1.600	1.940	0.027
Ce	0.010	0.950	1.410	1.940	10.300	0.640	0.650	1.300	1.830	2.220	0.023
Pr	0.070	0.110	0.150	0.180	0.720	0.090	0.090	0.150	0.180	0.190	0.016
Nd	0.050	0.380	0.500	0.550	2.060	0.050	0.240	0.460	0.610	0.670	0.091
Sm	0.010	0.020	0.050	0.050	0.210	0.010	0.010	0.020	0.050	0.060	0.105
Eu	0.001	0.010	0.010	0.010	0.040	0.002	0.005	0.010	0.010	0.010	0.029
Gd	0.010	0.020	0.030	0.050	0.270	0.010	0.010	0.020	0.050	0.050	0.110
Tb	<0.001	0.001	0.004	0.010	0.030	0.001	0.001	0.002	0.003	0.010	0.014
Dy	0.003	0.010	0.010	0.040	0.140	0.001	0.003	0.010	0.040	0.040	0.083
Ho	<0.001	0.001	0.005	0.010	0.040	0.001	0.001	0.003	0.010	0.010	0.020
Er	0.001	0.003	0.010	0.020	0.110	0.002	0.002	0.010	0.020	0.020	0.042
Tm	<0.001	0.001	0.010	0.010	0.010	0.001	0.001	0.010	0.010	0.010	0.013
Yb	0.001	0.002	0.004	0.030	0.060	0.001	0.002	0.004	0.020	0.030	0.050
Lu	<0.001	0.001	0.010	0.010	0.010	<0.001	<0.001	0.010	0.010	0.010	0.011
W	0.001	0.002	0.020	0.020	0.020	0.020	0.020	0.020	0.020	0.020	0.048
Pb	0.001	0.010	0.010	0.010	0.020	0.001	0.001	0.010	0.010	0.010	0.020
Th	<0.001	0.001	0.010	0.010	0.990	<0.001	<0.001	0.010	0.010	0.010	0.012
U	<0.001	<0.001	0.005	0.005	0.020	<0.001	<0.001	0.005	0.005	0.005	0.010

M.D.L.: Minimum Detection Limit. For each element, results below detection limit have been replaced with half the minimum detection limit from all analysis sections.

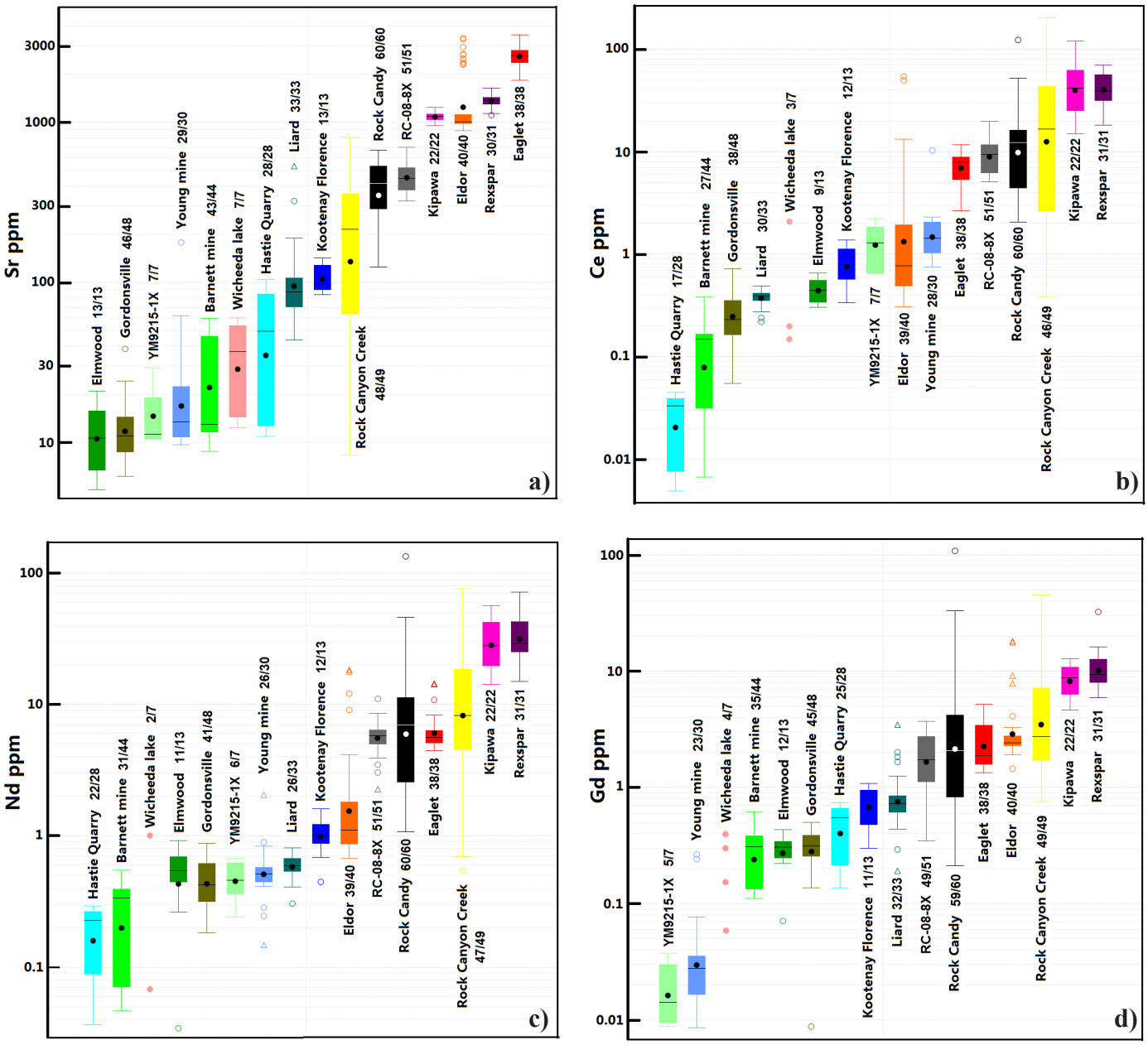

Fig. 4. Box plots of selected elements from fluorite of each deposit with the ratio of analyses above detection limit to total analyses. **a)** Sr; **b)** Ce; **c)** Nd; **d)** Gd; **e)** Yb; **f)** Y. Line: median value; solid dot: mean value; box: interquartile range (1st-3rd quartiles); open circle (outlier); farther than 1.5 x (1st-3rd quartiles); open triangle (outlier): farther than 3 x (1st-3rd quartiles); whiskers: extreme values that are not outliers. If there are less than five analyses above the detection limit, solid colour dots represent individual analyses.

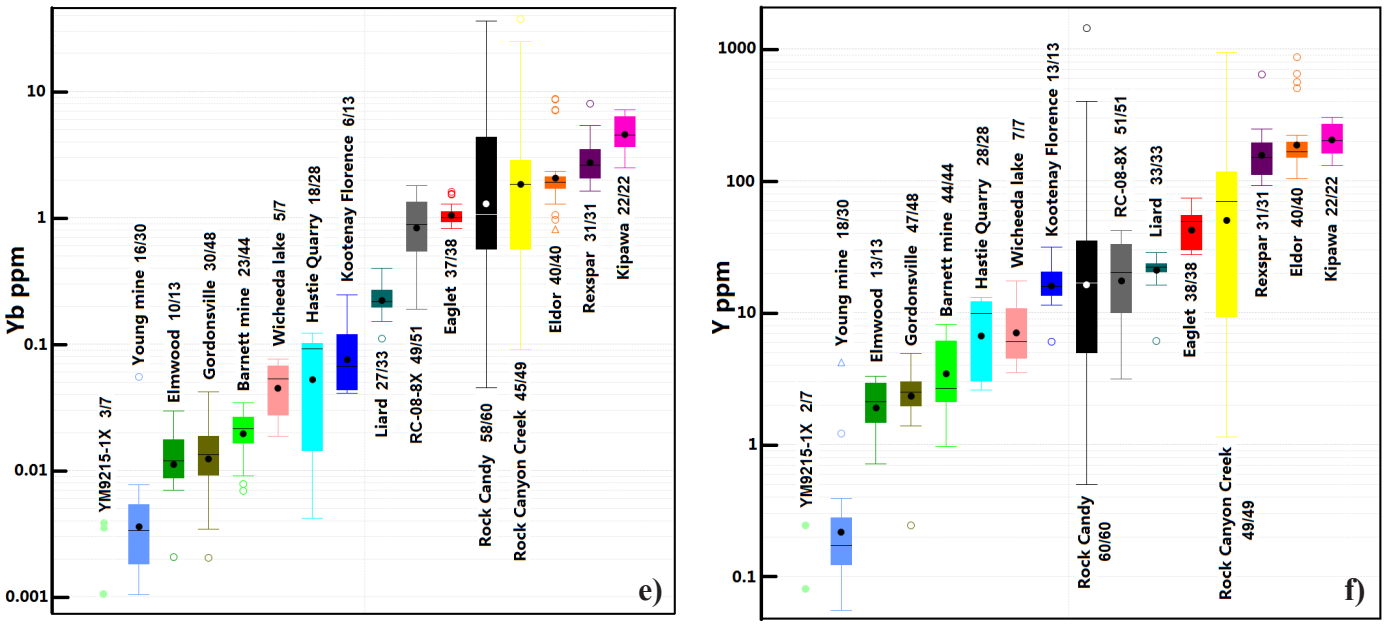

Fig. 4 continued. Box plots of selected elements from fluorite of each deposit with the ratio of analyses above detection limit to total analyses. **a)** Sr; **b)** Ce; **c)** Nd; **d)** Gd; **e)** Yb; **f)** Y. Line: median value; solid dot: mean value; box: interquartile range (1st-3rd quartiles); open circle (outlier); farther than 1.5 x (1st-3rd quartiles); open triangle (outlier): farther than 3 x (1st-3rd quartiles); whiskers: extreme values that are not outliers. If there are less than five analyses above the detection limit, solid colour dots represent individual analyses.

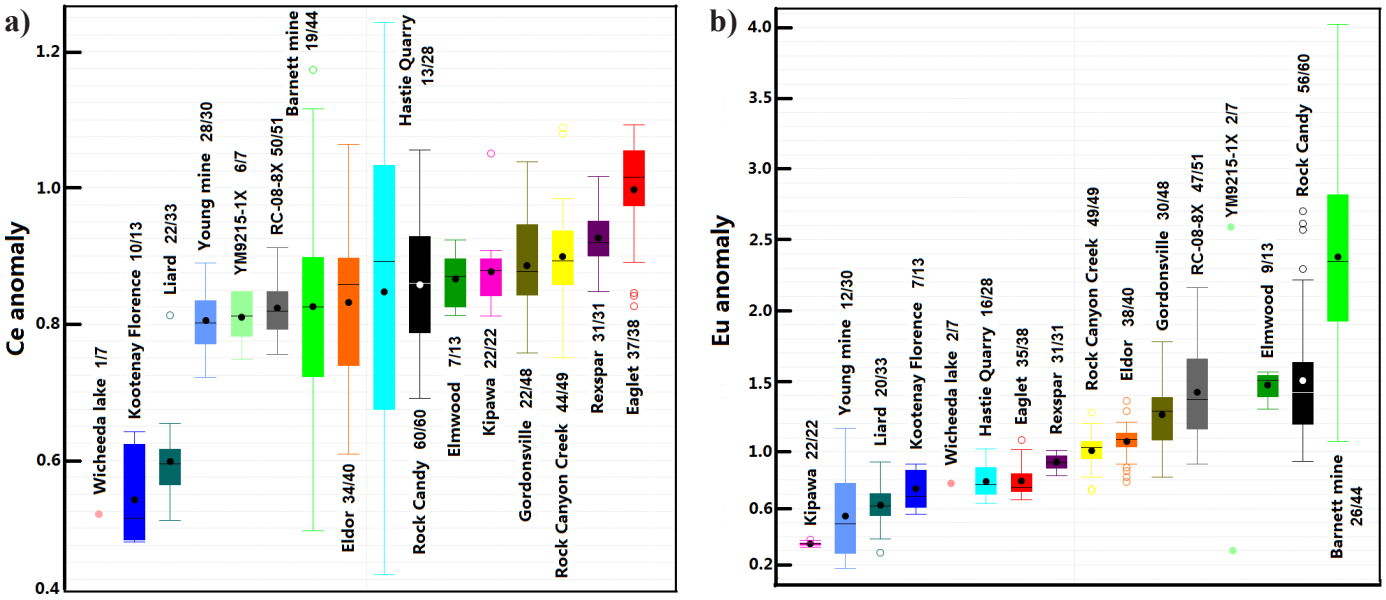

Fig. 5. Box plots of **a)** Ce anomalies and **b)** Eu anomalies from fluorite of each deposit. The ratios indicate the number of analyses for which anomalies could be determined, relative to the total number of analyses. Positive anomalies on these diagrams are higher than 1, conversely negative anomalies are lower than 1. Line: median value; solid dot: mean value; box: interquartile range (1st-3rd quartiles); open circle (outlier); farther than 1.5 x (1st-3rd quartiles); open triangle (outlier): farther than 3 x (1st-3rd quartiles); whiskers: extreme values that are not outliers. If there are less than five analyses above the detection limit, solid colour dots represent each individual analyses.

- The Eldor fluorite shows a large variation in La and progressively smaller variations in concentrations of Ce, Pr, Nd, Sm, and Eu (Figs. 4b, c, Fig. 6a; Table 3).
- Fluorite from Kipawa and Rexspar always has the highest contents (3rd quartile) of lanthanides except Eu; only Kipawa has prominent negative Eu anomalies (Figs. 4b, c, d, e, Fig. 5b; Fig. 6b).
- Hastie Quarry and Barnett mine fluorite has the lowest contents of La, Ce, Pr, and Nd (Figs. 4b, c, Fig. 6b; Table 3).
- Rock Candy and Rock Canyon Creek fluorite shows very wide ranges of lanthanide and Y concentrations (Figs. 4b, c, d, e, f; Figs. 6a, c).
- Elmwood and Gordonsville fluorite shows similar behaviors for all lanthanides and Y (Figs. 4b, c, d, e, f; Fig. 6c).
- The chondrite-normalized LREE contents of Young mine fluorite decreases from La to Eu (Fig. 6c).
- Fluorite from the Young mine contains the lowest concentrations of Eu, and many of analyses show that Eu contents are less than detection limits (Table 3).
- The chondrite-normalized patterns from Gd to Ho (excluding Y) of fluorite are flat in all deposits except for Elmwood, Gordonsville, and the Young mine (Fig. 6).
- Rexspar, Kipawa, Eldor, Rock Canyon Creek, Rock Candy, and Eaglet fluorite have flat or slightly negatively sloped chondrite-normalized patterns from Er to Lu, and their concentrations of Er, Tm, Yb, and Lu are elevated relative to those from other deposits in which the patterns from Er to Lu show a notable negative slope (Fig. 6).

Magnesium concentrations in fluorite are generally less than 10 ppm. Five to 45% of the analyses from each deposit contained detectable Mg, except for fluorite from Rock Canyon Creek (>60%). Detectable Mg concentrations in Rock Canyon Creek are between 2.10 (±0.26) – 582 (±47) ppm, and most are above 10 ppm (Table 3).

Manganese was detected in 20% of all the analyses. More than 85% of the analyses from Rexspar and Eaglet yielded between 2.92 (±0.14) and 7.96 (±0.39) ppm Mn, and fluorite grains from Eldor, Kipawa, Rock Candy, and Rock Canyon Creek contain detectable Mn, typically less than 10 ppm (Table 3).

Zirconium is detectable in 40% of all the analyses, and it is commonly present in concentrations less than 0.1 ppm. More than 85% of analyses from Liard have detectable Zr, ranging from 0.004 to 0.89 ppm. Approximately 75% of the analyses from Rock Canyon Creek contain Zr and have a large variation from 0.002 (±0.0003) to 11.3 (±0.9) ppm (Table 3).

More than half of all the analyses have detectable Ba, ranging from 0.001 (±0.0002) to 474 (±24) ppm, many of which are less than 1 ppm. Barium can be detected in 85% of analyses from Liard which has the highest content range (0.99 ±0.16 and 474 ±24 ppm). Barium is also commonly detected in concentrations above 1 ppm in fluorite from Rock Canyon Creek (60% detectable, 0.1 ±0.02 – 83.7 ±4.3 ppm) and Wicheeda Lake

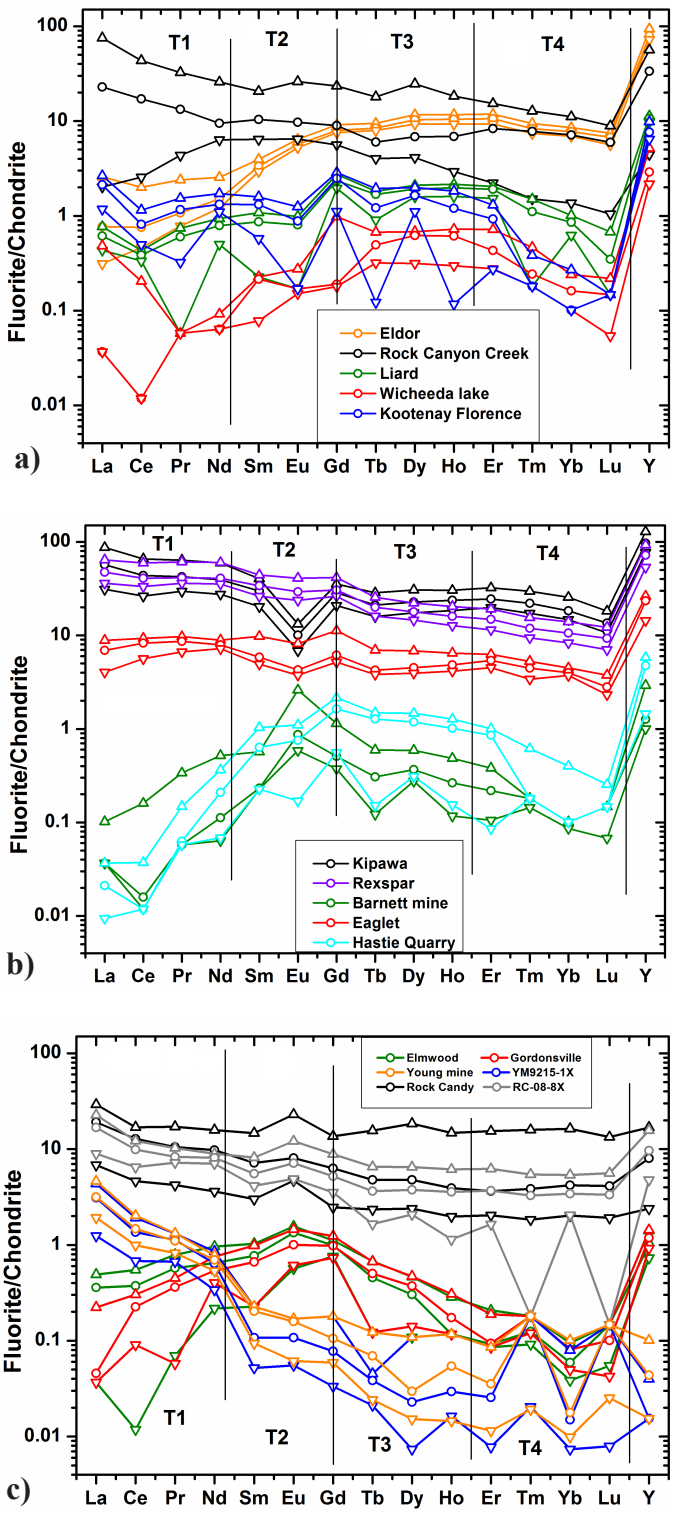

Fig. 6. Chondrite-normalized REE plots of fluorite for each deposit (chondrite data from Taylor and McLennan, 1985). **a)** Fluorite from Eldor, Rock Canyon Creek, Wicheeda Lake, Liard, and Kootenay Florence; **b)** Fluorite from Kipawa, Rexspar, Hastie Quarry, Barnett mine, and Eaglet; **c)** Fluorite from Rock Candy, RC-08-8X, Elmwood, Gordonsville, Young mine, and YM9215-1X. Lines split lanthanides into the four tetrads (McLennan, 1994). Solid line with open circle: median value; solid line with open downward triangle 1st quartile and upward triangle 3rd quartile.

(85% detectable, 0.63 ±0.10 – 5.84 ±0.93 ppm; Table 3).

Tungsten was detected in about half of all the analyses, although it rarely exceeds 1 ppm. Fluorite from Rexspar (90% detectable) has the highest W contents from 0.16 (±0.02) to 1.31 (±0.20) ppm. Fluorite from Kipawa has similar W contents (75% detectable, 0.14 ±0.02 – 0.57 ±0.09 ppm) to Rexspar. Eighty-two percent of fluorite analyses from Eaglet, and 63% from Eldor yield detectable concentrations of W, but values are rarely above 0.2 ppm. Fluorite from Rock Canyon Creek has detectable W in the 0.002 (±0.0003) to 0.71 (±0.1) ppm range. Detectable W is uncommon in other deposits (Table 3).

Thorium is detectable in 55% of all the analyses and concentrations are less than 1 ppm in most deposits. Rock Canyon Creek has the highest Th levels in fluorite (95% detectable analyses) with values ranging from 0.42 (±0.06) to 108 (±9) ppm (Table 3).

Uranium is detectable in more than 40% of all the analyses, mostly in concentrations less than 1 ppm. More than 85% of the analyses of Liard fluorite contain detectable U with values ranging from 0.7 (±0.15) to 6.75 (±0.92) ppm. The Liard fluorite has the highest U concentrations found in this study. The Rexspar deposit fluorite also has detectable U in 75% of the analyses (0.02 ±0.01 – 0.24 ±0.05 ppm). Fluorite samples from Rock Canyon Creek area also have a large range of U values, from 0.001 (±0.0002) to 3.22 (±0.44) ppm (Table 3).

Iron is detectable in most of the sample analyses, with concentrations ranging from 14.4 (±5.0) to 291 (±51) ppm. There are large overlaps in Fe concentrations between individual deposits. Twenty-five to seventy-seven percent of the analyses from Rock Canyon Creek show detectable levels of Sc, Ti, V, Nb, Mo, Ag, and Pb (Table 3). Other trace elements were not consistently detected in fluorite from the studied deposits.

3.2. Variation of trace elements within particular crystals

Numerous analyses of fluorite RC-08-8X and YM9215-1X were performed (Table 3) to test the homogeneity of trace elements in single fluorite crystals. Fifty sites were analyzed on the RC-08-8X crystal along two approximately perpendicular lines (a1-a18 and b1-b31, Fig. 2). Three compositional zones were identified along line a1-a18 (Fig. 7a). The first zone, from a1 to a5, contains lower Sr (320-420 ppm) and Ce (6 ppm), and higher Y (30-40 ppm), Gd (2-3 ppm), and Yb (1-2 ppm). The second zone, from a6 to a14, displays high Sr (450-650 ppm), varying Ce (10-20 ppm), and lower Y (8-20 ppm), Gd (1-2 ppm), and Yb (0.3-0.8 ppm). The third zone, from a15 to a18, has intermediate Sr and Y contents. Analytical line b1-b31 also shows three compositional zones (Fig. 7b). The first zone, from b1 to b11, has trace element contents that are between the compositions of the first and second zones on line a1-a18 (Fig. 7b). The second zone contains the highest Sr (500-700 ppm), highly variable Ce (5-16 ppm), and the lowest Y (3-25 ppm, mostly <10 ppm), Nd (2-5 ppm), Gd (0.3-2 ppm), and Yb (0.2-1.3 ppm), from b12 to b20. The third zone, from b21 to b31, contains the lowest Sr (320-400 ppm) and Ce (5-6 ppm), and the highest Y (30-40 ppm), Nd (5-6 ppm), Gd (2-3 ppm),

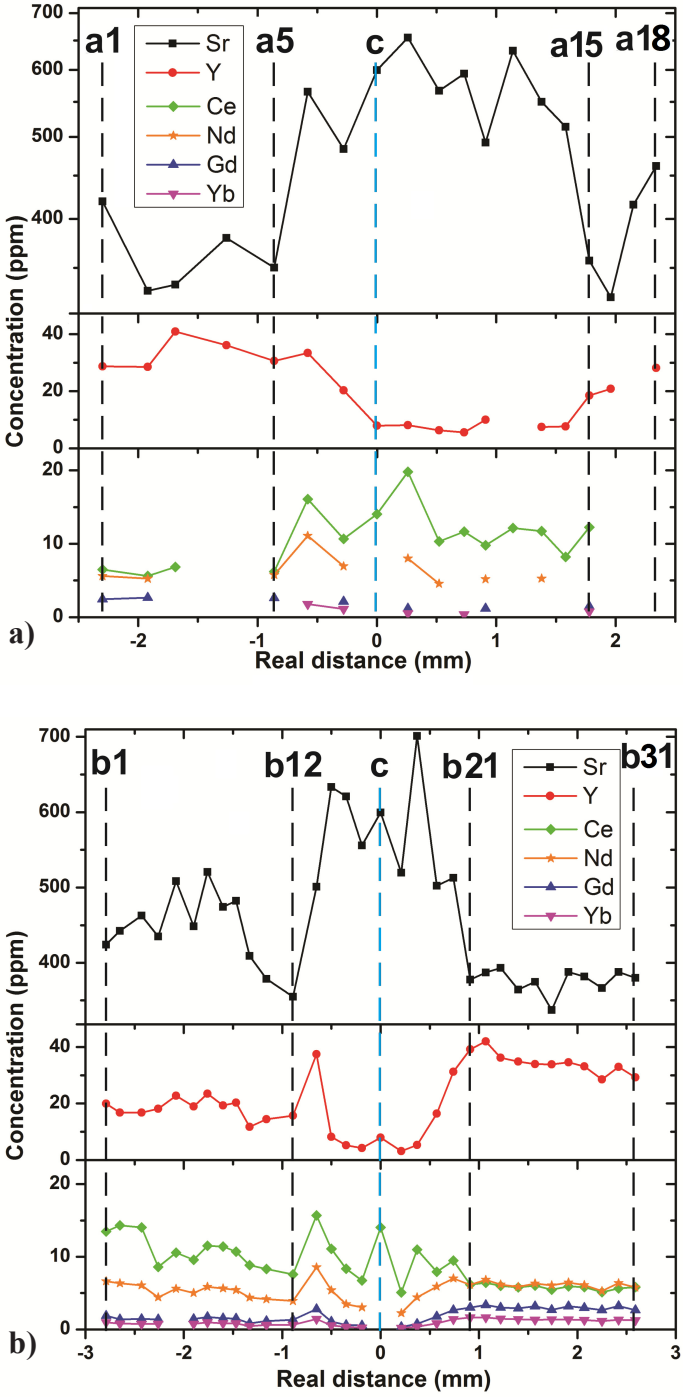

Fig. 7. Concentration variation of selected elements in fluorite along the analysis lines of RC-08-8X: **a)** line 'a1-a18' and **b)** line 'b1-b31' (see Fig. 2). The x axis represents the distances between the analytical points, '0' is the intersection point of the analytical lines, the 'c' point. Black dashed lines indicate the critical analytical points defining compositional zones, and blue dashed line indicates the central 'c' point (see also Fig. 2).

and Yb (1-2 ppm). In summary, the RC-08-8X crystal shown in Fig. 2 displays three compositional zones.

Because trace element concentrations are generally low in fluorite from the Young mine (Table 3), Sr, Ce, Pr, Nd, Tb,

and Er were selected to test for intra-grain variation (sample YM9215-1X). In the purple rim (Fig. 3) from d1 to d2, Sr and Tb contents decrease, whereas Ce, Pr, and Nd contents increase (Fig. 8). In the colourless zone from d3 to d4, Sr and Ce contents decrease, and Pr contents increase slightly. In the dark core from d5 to d7 (Fig. 3), the contents of Sr, Ce, Nd, and Tb show notable variations (Fig. 8), and Er content increases. More analyses would be required to establish a clear relationship between compositional and colour zonings

4. Discussion

Our discussion of the results will focus on comparing trace element concentrations in fluorite of specific deposits and groups of deposits, trace element variations within single fluorite crystals and the potential use of Rock Candy fluorite as a matrix-matched secondary standard.

4.1. Trace element composition of fluorite from individual deposits

For the purpose of this discussion, deposits under consideration can be divided into: 1) Sedimentary-hosted deposits (Liard, Hastie Quarry, Barnett mine, Young mine, Gordonsville, Elmwood, Kootenay Florence), 2) Peralkaline/alkaline rock-related deposits (Eaglet, Kipawa, Rexspar, Rock Candy, Rock Canyon Creek), and 3) Carbonatite-related deposits (Eldor, Wicheeda Lake).

Concentrations of Sr, Y, and lanthanides are consistently above LA-ICP-MS detection limits (Table 3) and show geochemical variations between deposits. To facilitate the comparisons between chondrite-normalized REE profiles, we adopted the 'tetrad' terminology as discussed by McLennan (1994), and Monecke et al. (2002). Lanthanides are divided into four tetrads: the 1st tetrad (T1) consists of La, Ce, Pr, Nd, the 2nd tetrad (T2) consists of Sm, Eu, Gd, the 3rd tetrad (T3) corresponds to Gd, Tb, Dy, Ho, and the 4th tetrad (T4) groups Er, Tm, Yb, Lu. Ratios between specific lanthanides, and lanthanide tetrads may be useful for constructing discrimination diagrams in addition to Ce and Eu anomalies and to Sr and Y contents,.

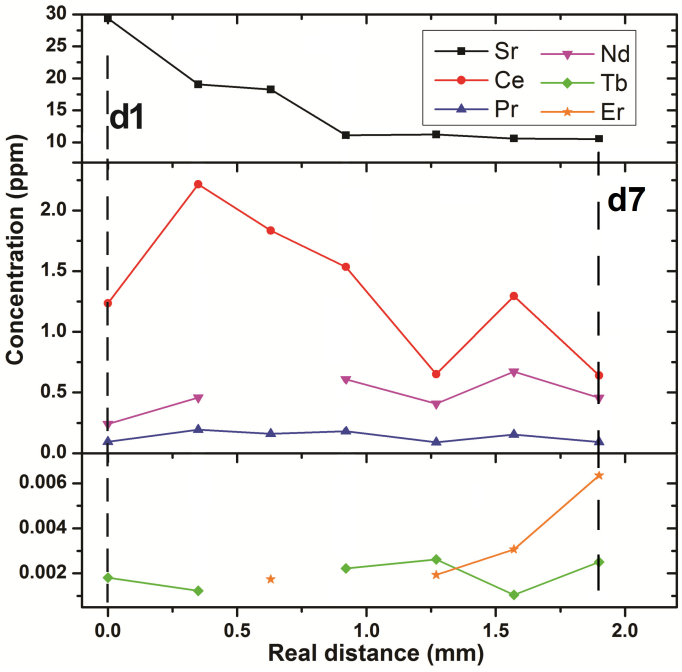

Fig. 8. Concentration variation of selected elements in fluorite along the analysis line of YM9215-1X. The '0' on the x axis is the analytical point on the edge of the crystal (d1, Fig. 3).

4.1.1. Trace element behaviors of fluorite from sedimentary-hosted deposits

Fluorite from sedimentary-hosted deposits has low trace element concentrations, which plot mostly below 3 on chondrite-normalized REE ratio diagrams (Fig. 6). Strontium concentrations are typically less than 200 ppm (Fig. 4a), and Y concentrations are all less than 31 ppm (Fig. 4f). All sedimentary-hosted fluorite, except from the Young mine, have nearly flat or convex-shaped chondrite-normalized REE patterns; flat or positively sloping T1, positively sloping T2, flat or negatively sloping T3, and negatively sloping T4 (Fig. 6; Table 5). The Young mine fluorite has a negatively sloping chondrite-normalized REE pattern, where T1 and T2 are notably negative, and T3 and T4 weakly negative.

The Hastie Quarry and the Barnett mine (Illinois-Kentucky mining district) both have convex shaped chondrite-normalized REE patterns, with strong positively sloping T1, positively sloping T2, flat T3, and negatively sloping T4 (Fig. 6b; Table 5). Hastie Quarry has negative Eu anomalies, whereas Barnett mine has the strongest positive Eu anomalies and largest Eu variation in this study (Fig. 5b). Due to the lack of detailed geological information for Barnett mine, the origin of the high Eu source is unclear. However, Eu enrichment is generally associated with changes of oxidation state (Möller and Holzbecher, 1998; Bau et al., 2003).

The Elmwood and Gordonsville deposits (central Tennessee zinc district) both have similar convex chondrite-normalized REE patterns with positive slopes in T1, T2, and negatively sloping T3 and T4 (Table 5). The negatively sloping T3 is distinct from the flat T3 of most other deposits (Fig. 6; Table 5). The Elmwood and Gordonsville deposits are only a few kilometres apart (Lewchuk, 1996), and are likely to have formed from fluid of the same composition and similar temperatures.

Liard (carbonate/shale-hosted fluorite±witherite±barite deposit) and Kootenay Florence (sedimentary-related Ag-Pb-Zn deposit) both have generally flat to slightly convex shape chondrite-normalized REE patterns with similar REE contents (Fig. 6a). Tetrad patterns, T1 and T3 are flat, T2 is positively sloping and T4 is negatively sloping. Unlike the other sedimentary-hosted (MVT) deposits discussed above, Liard and Kootenay Florence are not close to each other (Fig. 1).

The Young mine (Eastern Tennessee zinc district) is the only deposit that shows enriched LREE and depleted HREE (all tetrads are negative; Table 5, Fig. 6c). The reason for this

distinct chondrite-normalized REE pattern is unclear due to the lack of available information.

4.1.2. Trace element behaviors of fluorite from peralkaline/alkaline-related deposits

Fluorite from peralkaline/alkaline rock-related deposits have chondrite-normalized ratios higher than 2 (Fig. 6, Table 5), and Sr contents higher than 100 ppm, except for Rock Canyon Creek (Fig. 4a). Eaglet, Kipawa, Rexspar, Rock Candy are relatively flat in T1, have flat or weakly sloping T2 and T3 with variable Eu anomalies, and weakly negative or positive T4 slopes. The La to Nd of the Rock Canyon Creek fluorite displays negative T1 and T2 slopes.

Fluorite from Kipawa and Rexspar has higher lanthanide contents than other deposits, and they have similar chondrite-normalized REE patterns, with the exception of Eu anomalies (Fig. 6b). Rexspar fluorite is commonly hosted by tuffaceous trachyte with pervasive potassic alteration (Pell 1992). The Rexspar fluorite has a flat chondrite-normalized REE pattern with weakly negative Eu anomalies. This pattern is similar to those of fluorite from alkaline rocks (Gagnon et al., 2003). Kipawa fluorite has a flat chondrite-normalized REE pattern, with a strong negative Eu anomaly. The fluorite REE pattern is very similar to the syenite REE pattern in this region (Currie and Van Breemen, 1996), suggesting that the fluorite is directly related to the syenite nearby.

Rock Candy (fluorite ±barite vein) and Eaglet (Mo- and fluorite-bearing) are deposits related to alkaline rocks (Table 1). They have flat chondrite-normalized REE patterns and lower REE contents than Rexspar and Kipawa (Figs. 6b, c). Their tetrad patterns are similar to Rexspar and Kipawa with the exception of a weakly positive T4 for Rock Candy fluorite. Rock Candy has wide ranges of REE and Y contents (Figs. 4b, c, d, e, f) with notably positive Eu anomalies (Fig. 5b), and varying Y relative to HREE (Fig. 6c). This variation may reflect the evolution of fluid composition or change in temperature over time (Bau and Dulski, 1995). Positive Eu anomalies of fluorite are usually associated with enriched Eu hydrothermal fluids. The Eaglet fluorite has negative Eu anomalies (Fig. 5b) and prominent high Sr concentrations (Fig. 4a). The elevated Sr contents are likely due to high Sr contents in fluid suggested by co-existing celestite in mineralized zones (Hora et al., 2008). The flat or nearly flat chondrite-normalized REE patterns in the four deposits are similar to the REE patterns of fluorite associated with alkaline rocks at Gallinas Mountains (Gagnon et al., 2003).

Rock Canyon Creek deposit contains disseminated and fine veinlet fluorite hosted by dolostone. Although, no igneous rocks outcrop (Pell and Hora, 1987; Samson et al., 2001), mineralization may be carbonatite or peralkaline intrusion-related (Pell and Hora, 1987). The presence of Al-F minerals (cyrolite and prosopite) in float has been taken as evidence of an alkaline rock association (Samson et al., 2001). Fluorite from Rock Canyon Creek shows large variations in Sr, Y, and lanthanides (Figs. 4, 6a). The chondrite-normalized REE patterns show a very wide range (especially in the LREE), lack Eu anomalies, and have a weakly negative slope; however, the median values show a weak sinusoidal shape. These variations in trace element concentrations probably reflect the difference in origin between fluorite from the main zone and the float of unknown provenance.

4.1.3. Trace element behaviors of fluorite from carbonatite-related deposits

Fluorite from carbonatite-related deposits has widely varying trace element contents. The chondrite-normalized REE patterns show sinusoidal shapes. They both have wide content ranges for T1, positively sloped T2, weakly positively sloped or flat T3, and negatively sloped T4 (Fig. 6a; Table 5).

Fluorite at Eldor may contain intergrown monazite and aggregated bastnaesite (Wright et al 1998; Gagnon et al., 2012). It is enriched in HREE (and Y) and depleted in LREE (Fig. 6a). The fluorite shows large variations in concentrations of La, Ce, Pr, and Nd relative to HREE. The depletion of LREE in fluorite from Eldor may be due to preferential incorporation of LREE into monazite and bastnaesite, relative to fluorite. Furthermore, the large range of negative Ce anomalies in Eldor fluorite (Fig. 5a) may be explained by the effect of a change in oxidation-reduction conditions as fluorite crystallization progressed. At the Wicheeda Lake carbonatite, fluorite is only a local accessory mineral (Trofanenko et al., 2014). There are not enough data to make a concrete interpretation for the Wicheeda Lake fluorite and this is reflected in the erratic relationship between upper and lower quartiles on figure 6a. Concentrations of REE are in the same range as fluorites from sedimentary-hosted deposits (Fig. 6). But, the wide variations of LREE contents and sinusoidal shapes of REE patterns are similar to the carbonatite-related deposit, Eldor.

4.1.4. Characteristics of other trace elements

Magnesium, Mn, Zr, Ba, W, Th, and U in fluorite have rarely been reported in the literature, due to their very low abundances in the mineral, but the presence of these elements in detectable concentrations may be specific to some deposit types. For example, Rock Canyon Creek fluorite has very high concentrations of ‘uncommon’ trace elements including Mg, Mn, Pb, Th, V, Nb, Mo, Sc, W, Zr, and Ba (Table 3). In Liard fluorite, the Ba varies from 0.01 to 474 ppm; and U from 0.01 to 6.75 ppm (Table 3). This fluorite crystallized from the same fluid as co-existing witherite and barite (Changkakoti et al., 1987), explaining its high Ba content. The fluid may have been similar to modern waters at Liard Hot springs which are slightly radioactive (Holland, 1955) explaining detectable U content in fluorite.

4.2. Trace element variations in single crystals vs. multiple crystals of the same deposit

Sample RC-08-8X is a single crystal (Fig. 2) from Rock Candy, a vein type deposit (Table 1). This sample has no visually identifiable zoning and was analyzed 50 times. The

Table 4. The compositional variations for analyses in each zone of sample RC-08-8X, and analytical variations from NIST 613 and 615 through all analyses. All values in percent unless otherwise indicated.

	Sr	Y	La	Ce	Pr	Nd	Sm	Eu	Gd	Tb	Dy	Ho	Er	Tm	Yb	Lu
Zone 1: a1-a5, b21-b31, 16 analyses	13.0	25.1	23.1	14.5	13.9	14.9	16.9	11.4	19.2	16.8	18.8	25.4	28.3	30.5	22.7	24.0
Zone 2: a6-a14, c, b13-b20, 18 analyses	21.9	171.4	63.9	63.1	81.6	81.8	107.4	84.1	124.5	135.9	148.8	131.5	184.2	101.4	141.4	108.5
Zone 3: a15-a18, b1-b12, 16 analyses	26.1	41.6	34.5	41.1	40.1	34.1	39.1	46.2	37.0	25.5	36.6	33.9	37.3	30.7	38.8	33.9
Precision from NIST 613	5.0	8.1	6.3	5.5	5.5	6.4	6.2	5.7	7.1	6.9	7.9	8.2	8.7	8.0	7.3	8.8
Precision from NIST 615	16.7	18.7	15.9	26.3	14.3	19.1	19.4	12.7	20.9	10.7	15.8	12.8	16.9	12.0	15.6	12.4

The compositional variations are determined by 2 x standard deviation divided by average value.

Table 5. The characteristics of chondrite-normalized REE plots for each deposit.

Deposit name	Lanthanide/Chondrite	General pattern	Ce anomalies	Eu anomalies	T1 shape	T2 shape	T3 shape	T4 shape
Sedimentary-hosted:								
Liard	3rd quartile <3	Nearly flat, very weak convex	- - -	- -	Flat	+ +	Flat	- -
Kootenay Florence	3rd quartile <3	Nearly flat, very weak convex	- - -	- -	Flat	+ +	Flat	- -
Hastie Quarry	3rd quartile <3	Convex	- - Wide range	- -	+ + +	+ +	Flat	- -
Barnett mine	3rd quartile <3	Convex	- - Wide range	+ + + Wide range	+ + +	+ +	Flat	- -
Elmwood	3rd quartile <2	Convex	- -	+ + +	+ +	+ +	- -	- -
Gordonsville	3rd quartile <2	Convex	- -	+ +	+ +	+ +	- -	- -
Young mine	3rd quartile <3 except La	Negative slope, enriched LREE	- -	- -	- -	- -	-	-
Peralkaline/alkaline-related:								
Kipawa	1st quartile >6	Nearly flat, very weak negative slope	- -	- - -	Nearly flat (-)	Flat	Flat	-
Rexspar	1st quartile >7	Nearly flat, very weak negative slope	-	-	Flat	Flat	Flat	-
Eaglet	1st quartile >2	Nearly flat, very weak negative slope	No anomaly	- -	Flat	Nearly flat (+)	Flat	-
Rock Candy	1st quartile >2	Nearly flat, very weak negative slope	- - Wide range	+ +	Nearly flat (-)	Nearly flat (-)	Flat	+
Rock Canyon Creek	1st quartile >2	Weak negative slope	- -	No anomaly	Undetermined	Nearly flat (-)	Flat	-
Carbonatite-related:								
Eldor	0.4<1st quartile, 3rd quartile<10.4	Sinusoidal	- - Wide range	+	Undetermined	+ +	+	-
Wicheeda lake[1]	0.06<1st quartile, 3rd quartile<10	Sinusoidal	- - -	- -	Undetermined	+ +	Flat	- -

Positive and negative anomalies or slope are indicated by '+' and '-'. A single notation (e.g. +) refers to a 'weak' signature, double notation (e.g. ++) refers to a 'medium' signature and triple notation refers to a 'strong' signature. [1] The Wicheeda Lake sample has only one analysis showing a Ce anomaly, and two analyses showing Eu anomalies.

results obtained from this sample are compared with 61 analyses from 35 different Rock Candy grains (Fig. 4; Fig. 6c). The compositional ranges of Sr, Y, La, Ce, Pr, Nd, Sm, Eu, Gd, and Yb, constrained by the 1st and 3rd quartile concentrations, show that variations within a single grain are less than those of multiple grains from the same deposit. The 1st quartile values are less than those of multiple grains from the same deposit for Tb, Dy, Ho, Er, Tm, and Lu in sample RC-08-8X (Fig. 6c). The blank signal of some analyses for sample RC-08-8X generated very high background signals (e.g., 0-1,000 counts-per-seconds vs. 0-250 counts-per-seconds, for Tm) resulting in high detection limits affecting ~10-30% of analyses for Tb, Dy, Ho, Er, Tm, and Lu. In our statistical representation of the data, the analyses less than the detection limit are replaced by half of the minimum detection limit (M.D.L./2), thus the true contents of some elements in RC-08-8X may be underestimated. To exaggerate this point, when comparing all detectable analyses (without filtering via detection limits) of Tm and Lu, the 1st and 3rd quartiles of RC-08-8X are all within the1st and 3rd quartile range of the Rock Candy fluorite (Figs. 9a, b). For Rock Candy fluorite, the intra-grain trace element variations are smaller than those from multiple fluorite grains.

Sample YM9215-1X is a single crystal with visible colour zoning (Fig. 3) from the Young mine, a MVT deposit (Table 1). We compare 7 analyses of this crystal to other Young mine grains (30 analyses from 9 grains). For Sr, La, Ce, Pr, Nd, Sm, Gd, and Tb, the total concentration variation of each element in YM9215-1X is less than the Young mine fluorite (Table 3), however the ranges of the 1st and 3rd quartiles are greater (Fig. 6c). The same comparison of 1st and 3rd quartile ranges cannot be applied for Y, Eu, Dy, Ho, Er, Tm, Yb, and Lu, because more than 40% of the data are below the detection limit in all the Young mine samples, causing the 1st quartile values to be unreliable. However, the 3rd quartile values show that the contents of Y, Eu, Dy, Ho, Er, Tm, Yb, and Lu in sample YM9215-1X are less than other Young mine grains. Although the elemental variations for YM9215-1X are not restricted within variations for the Young mine fluorite, the chondrite-normalized REE patterns are similar (Fig. 6c), as expected. These results show that intra-grain trace element variations are small when elemental concentrations are notably higher than the detection limits. But, when element concentrations are close to the detection limits, the intra-grain trace element variations are close to or larger than variations between multiple grains. One cause of this could be the relatively large uncertainty associated with low precision and high detection limits. For this reason, it

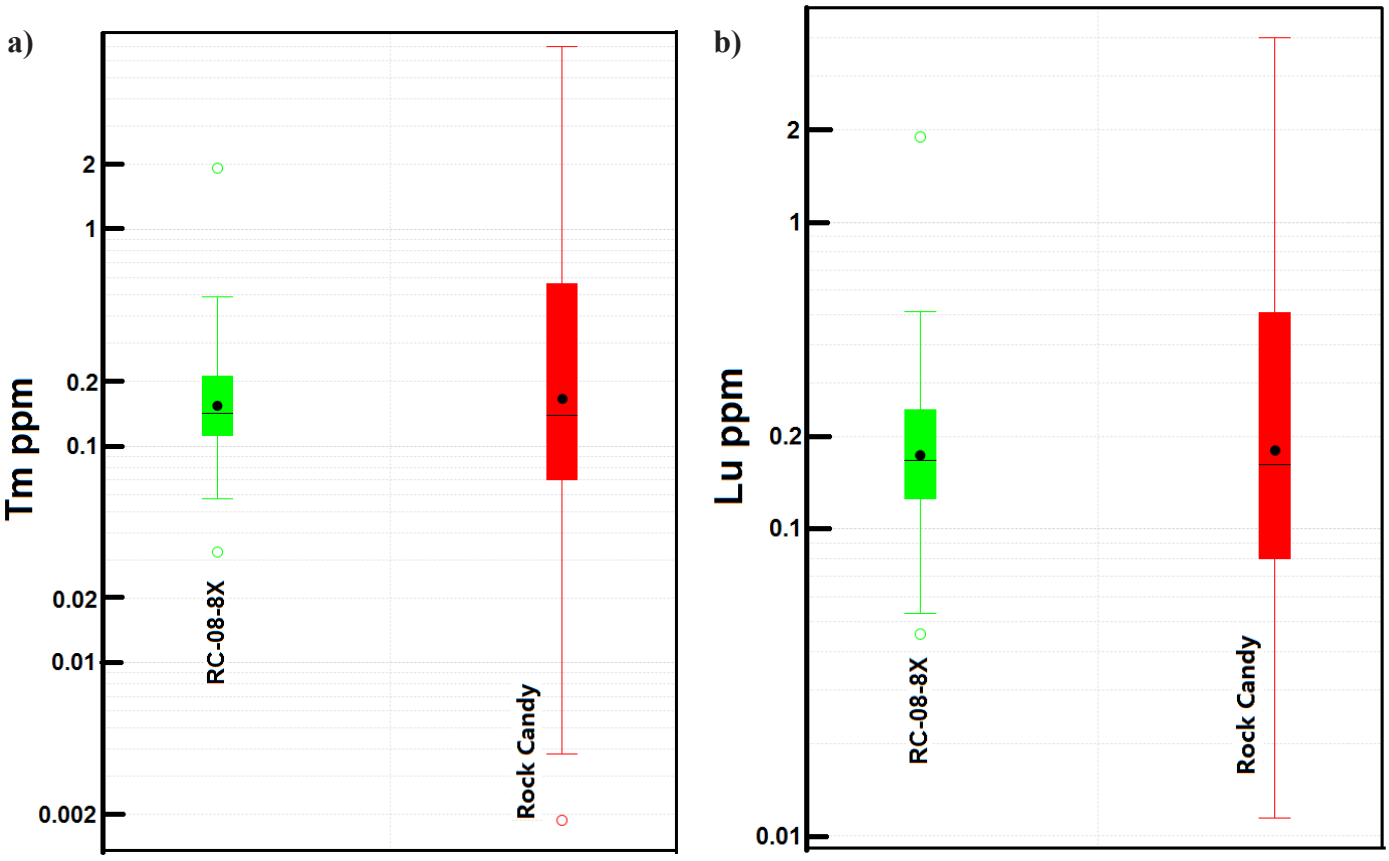

Fig. 9. Box plots of **a)** Tm and **b)** Lu from RC-08-8X and other Rock Candy fluorite with all analyses including those less than the detection limits. For Tm, high detection limits were determined for 30% of all analyses and are between 0.14-0.49 ppm. For Lu, high detection limits were determined for 25% of all analyses and are between 0.11-0.51 ppm. Line: median value; solid dot: mean value; box: interquartile range (1st-3rd quartiles); open circle (outlier); further than 1.5 x (1st-3rd quartiles); whiskers: extreme values that are not outliers.

is important to take note of the uncertainty for analyses that are close to the detection limit.

4.3. Potential use of Rock Candy fluorite as a matrix-matched secondary standard for LA-ICP-MS

The fractionation indices of elements in NIST glass differ substantially from those of the internal standard, so non-negligible error may be introduced (Jackson, 2008; Sylvester, 2008). When NIST glass is used to calibrate fluorite analyses, a matrix-matched secondary standard enhances quality-control. Unfortunately, a commercial synthetic fluorite standard is currently unavailable, and natural minerals are rarely homogeneous. The LA-ICP-MS, results from crystal RC-08-8X indicate three zones defined by Sr, Y, and lanthanides (Figs. 2, 7). Most of the compositional variations (2σ) in Zone 1 are less than 20%, and all are less than 30.5% (Table 4). With the exception of Sr, the analyses of all elements considered in Zone 2 have 2σ above 60% (Table 4, Fig. 7).The compositional variations of Zone 3 range between 25%-45%. Comparing Zone 1 with NIST 613, the compositional variations for Sr (328-419 ppm, 13%) and Y (28-41 ppm, 25%) are approximately three times higher than the analytical variations (determined precision, Sr ppm, 5%; Y ppm, 8%). The concentrations of lanthanides in Zone 1 are similar to NIST 615, and many of the compositional variations are comparable to the analytical variations (Table 4). The small compositional variations detected in Zone 1 of the RC-08-8X make it a candidate for a matrix-matched secondary standard. The adjacent areas, between the a1-a5 and b21-b31 lines, are currently the best option for use as a matrix-matched secondary standard.

5. Summary

Fluorite from sedimentary-hosted deposits (Liard, the Hastie Quarry, the Barnett mine, the Young mine, Gordonsville, Elmwood, Kootenay Florence) can be characterized by lanthanide/chondrite ratios <3, convex or negatively sloped REE patterns, negatively sloped T4, and low concentrations of Sr, Y, and lanthanides. Fluorite from peralkaline/alkaline rock-related deposits (Eaglet, Kipawa, Rexspar, Rock Candy, Rock Canyon Creek) mainly show elevated Sr, Y, and lanthanide contents and lanthanide/chondrite >2, flat to weakly negative sloping patterns on REE chondrite-normalized plots and weakly sloping T4. Fluorite from carbonatite-related deposits (Eldor, Wicheeda Lake) has sinusoidal REE chondrite-normalized patterns, with wide ranges of LREE contents. High concentrations of other elements such as Ba, Th, and U are distinctly related to particular deposits (Rock Canyon Creek and Liard).

Trace elemental variations in single fluorite crystals are less than the variations between crystals from the same deposit, and are unlikely to significantly affect the use of fluorite trace element contents to distinguish deposits. Detailed analyses of single fluorite crystals revealed compositional zoning regardless of presence or absence of visible zoning. A compositional zone was identified in a fluorite crystal (RC-08-8X) from Rock Candy that could be used as a matrix-matched secondary standard for fluorite. A larger data compilation is required to produce valid discrimination diagrams.

Acknowledgments

This project was partly funded by the Targeted Geoscience Initiative 4 (TGI4), a Natural Resources Canada programme carried out under the auspices of the Geological Survey of Canada in collaboration with the British Columbia Geological Survey. Samples from the Cave-in-Rock District were collected by F. Brett Denny and Zak Lasemi of the Illinois State Geological Survey, Prairie Research Institute, IL. Samples from the Tennesse MVT deposits were donated by Jason K. Dunning of Nyrstar US Inc., Fort Lauderdale, FL. The Eldor samples were provided by Daren Smith of Dahrouge Geological Consulting Ltd., Edmonton, AB. Access to the drill core from the Wicheeda Lake carbonatite was provided by Chris Graf of Spectrum Mining Corporation, Wardner, BC. Matamec Explorations Inc., and Frédéric Fleury (Gestion Aline Leclerc, Inc,) are thanked for their hospitality at the Zeus project (Kipawa).

References cited

Allan, J.F., 1992. Geology and Mineralization of the Kipawa Yttrium-Zirconium Prospect, Quebec. Exploration Mining and Geology, 1, 283-295.

Alvin, M.P., Dunphy, J.M. and Groves, D.I., 2004. Nature and genesis of a carbonatite-associated fluorite deposit at Speewah, East Kimberley region, Western Australia. Mineralogy and Petrology, 80, 127-153.

Andrade, F.R.D., Möller, P., Lüders, V., Dulski, P., and Gilg, H.A., 1999. Hydrothermal rare earth elements mineralization in the Barra do Itapirapuã carbonatite, southern Brazil: behaviour of selected trace elements and stable isotopes (C,O). Chemical Geology, 155, 91-113.

Baele, J-M., Monin, L., Navez, J., and André, L., 2012. Syetematic REE partitioning in cubo-dodecahedral fluorite from Belgium revealed by cathodoluminescence spectral imaging and laser ablation-ICP-MS. In: Broekmans, M. A. T. M. (Ed.), Proceedings of the 10th International Congress for Applied Mineralogy, 23-30.

Bailey, A.D., Hunt, R.P., and Taylor, K.N.R., 1974. An ESR study of natural fluorite containing manganese impurities. Mineralogical Magazine, 39, 705-708.

Bau, M. and Dulski, P., 1995. Comparative study of yttrium and rare-earth element behaviours in fluorine-rich hydrothermal fluids. Contributions to Mineralogy and Petrology, 199, 213-223.

Bau, M., Romer, R.L., Lüders, V., and Dulski, P., 2003. Tracing element sources of hydrothermal mineral deposits: REE and Y distribution and Sr-Nd-Pb isotopes in fluorite from MVT deposits in the Pennine Orefield, England. Mineralium Deposita, 38, 992-1008.

Baxter, J.W., Bradbury, J.C., and Hester, N.C., 1973. A Geologic Excursion to Fluorspar Mines in Hardin and Pope Counties, Illinois. Illinois State Geological Survey, Guidebook Series II, 28p.

Bettencourt, J.S., Leite Jr., W.B., Goraieb, C.L., Sparrenberger, I., Bello, R.M.S. and Payolla, B.L., 2005. Sn-polymetallic greissen-type deposits associated with late-stage rapakivi granites, Brazil: fluid inclusion and stable isotope characteristics. Lithos, 80, 363-386.

Bill, H. and Calas, G., 1978. Color centers, associated rare-earth ions and the origin of coloration in natural fluorites. Physics and Chemistry of Minerals, 3, 117-131.

Borrok, D.M., Kesler, S.E., Boer, R.H., and Essene, E.J., 1998. The Vergenoeg Magnetite-Fluorite Deposit, South Africa: Support for a Hydrothermal Model for Massive Iron Oxide Deposits. Economic Geology, 93, 564-586.

Bosze, S. and Rakovan J., 2002. Surface-structure-controlled sectoral zoning of the rare earth elements in fluorite from Long Lake, New York, and Bingham, New Mexico, U.S.A. Geochimica et Cosmochimica Acta, 66, 997-1009.

Cardellach, E., Canal, A., and Grandia, F., 2002. Recurrent hydrothermal activity induced by successive extensional episodes: the case of the Berta F-(Pb-Zn) vein system (NE Spain). Ore Geology Reviews, 22, 133-144.

Changkakoti, A., Gray, J., and Morton, R.D., 1987. The role of basinal brines and thermal springs in the genesis of carbonate-hosted fluorite-witherite mineralization in the Liard river area, British Columbia, Canada. Neues Jahrbuch für Mineralogie. Monatshefte, 5, 217-232.

Chesley, J.T., Halliday, A.N., Kyser, T.K., and Spry, P.G., 1994. Direct dating of Mississippi Valley-type mineralization: Use of Sm-Nd in fluorite. Economic Geology, 89, 1192-1199.

Cunningham, C.G., Rassmussen, J.D., Steven, T.A., Rye, R.O., Rowley, P.D., Romberger, S.B. and Selverstone, J., 1998. Hydrothermal uranium deposits containing molybdenum and fluorite in the Marysvale volcanic field, west-central Utah. Mineralium Deposita, 33, 477-494.

Currie, K.L. and Van Breemen, O., 1996. The origin of rare minerals in the Kipawa syenite complex Western Quebec. The Canadian Mineralogist, 34, 435-451.

Deer, W.A., Howie, R.A., and Zussman, J., 1965. Rock-forming minerals. Halsted Press, London, 347-353.

Deng, X., Chen, Y., Yao, J., Bagas, L., and Tang, H., 2014. Fluorite REE-Y (REY) geochemistry of the ca. 850 Ma Tumen molybdenite-fluorite deposit, eastern Qinling, China: Constraints on ore genesis. Ore Geology Reviews, 63, 532-543.

Denny, F.B., and Counts, R.C., 2009. Bedrock Geology of Shetlerville Quadrangle, Pope and Hardin Counties, Illinois: Illinois State Geological Survey, STATEMAP, Shetlerville-BG, 1:24,000 scale; report, 6p.

Dimitrova, D., Mladenova, V., and Vassilkyoka, R., 2011. LA-ICP-MS study of fluorite from the Lukina Padina deposit, NW Bulgaria. Bulgarian Geological Society, National Conference with international participation "GEOSCIENCES 2011", 15-16.

Eppinger, R.G., and Closs, L.G., 1990. Variation of trace elements and rare earth elements in fluorite: A possible tool for exploration. Economic Geology, 85, 1896-1907.

Fourie, P.J., 2000. The Vergenoeg fayalite Fe-oxide fluorite deposit, South Africa: some new aspects. In: Porter, T.M. (Ed.), Hydrothermal Fe-oxide copper–gold and related deposits: a global perspective. Australian Mineral Foundation, Adelaide, pp. 309–320.

Fyles, J.T., 1967. Geology of the Ainsworth-Kaslo area, British Columbia. British Columbia Geological Survey Bulletins, 53.

Gagnon, J.E., Samson, I.M., Fryer, B.J., and Williams-Jones, A.E., 2003. Compositional heterogeneity in fluorite and the genesis of fluorite deposits: Insights from LA-ICP-MS analysis. The Canadian Mineralogist, 41, 365-382.

Gagnon, G., Rousseau, G., Camus, Y., and Gagné, J., 2012. NI 43-101 Technical Report, Preliminary Economic Assessment: Ashram rare earth deposit for Commerce Resources Corporation. <http://www.commerceresources.com/assets/docs/reports/2015-01-07_GG-PEA-Report.pdf> Accessed on 12th Sep. 2015.

Grogan, R.M., and Bradbury, J.C., 1967. Origin of the stratiform fluorite deposits of southern Illinois. Economic Geology Monograph, 3, 40-51.

Grogan, R.M., and Bradbury, J.C., 1968. Fluorite-zinc-lead deposits of the Illinois-Kentucky mining district. In: Ridge, J.D., (eds.), Ore deposits of the United States, 1933–1967: New York. American Institute of Mining, Metallurgy, and Petroleum Engineers, pp. 370–399.

Hagni, R.D., 1999. Mineralogy of beneficiation problems involving fluorspar concentrates from carbonatite-related fluorspar deposits. Mineralogy and Petrology, 67, 33-44.

Hill, G.T., Campbell, A.R., and Kyle, P.R., 2000. Geochemistry of the southwestern New Mexico fluorite occurrences, implications for precious metals exploration in fluorite-bearing systems. Journal of Geochemical Exploration, 68, 1-20.

Holland, S.S., 1955. Fluorite-Witherite: Gem; B.C. Minister of Mines, Annual Report 1954, A178-179.

Hora, Z.D., Langrova, A., and Pivec, E., 2008. Eaglet property revisited: fluorite-molybdenite porphyry-like hydrothermal system, east-central British Columbia (NTS 093A/10W). Geological Fieldwork 2007, British Columbia Geological Survey, 17-30.

Jackson, S.E., 2008. Calibration strategies for elemental analysis by LA-ICP-MS. In: Sylvester, P. (Eds.), Laser Ablation–ICP–MS in the Earth Sciences current practices and outstanding issues. Mineralogical Association of Canada Short Course 40, Vancouver, B.C., pp. 169-188.

Jochum, K.P., Weis, U., Stoll, B., Kuzmin, D., Yang, Q., Raczek, I., Jacob, D.E., Stracke, A., Birbaum, K., Frick, D.A., Günther, D., and Enzweiler, J., 2011. Determination of Reference Values for NIST SRM 610–617 Glasses Following ISO Guidelines. Geostandards and Geoanalytical Research, 35, 397-429.

Kesler, S.E., Gesink, J.A. and Haynes, F.M., 1989. Evolution of mineralizing brines in the east Tennessee Mississippi Valley-type ore fields. Geology, 17, 466-469.

Klemme, S., Prowatke, S., Münker, C., Magee,C., Lahaye, Y., Zack, T., Kasemann, A., Cabato, E.J. and Kaeser, B., 2008. Synthesis and preliminary characterization of new silicate, phosphate and titanite reference glasses. Geostandards and Geoanalytical Research, 32, 39-54.

Kogut, A.I., Hagni, R.D., and Schneider, G.I.C., 1998. Geology, mineralogy, and paragenetic sequence of the Okorusu carbonatite-related fluorite ores, Namibia. In: Schweizerbart'sche, E. (Ed.), Proceedings of the Quadrennial IAGOD Symposium, 9, pp. 555-573.

Levresse, G., Trittla, J., Villareal, J. and González-Partida, E., 2006. The "El Pilote" fluorite skarn: A crucial deposit in the understanding and interpretation of the origin and mobilization of F from northern Mexico deposits. Journal of Geochemical Exploration, 89, 205-209.

Lewchuk, M.T., 1996. Genesis of the central Tennessee Mississippi Valley-type ore deposits and host rock dolomitization from Paleomagnetism. Digitized Theses, Paper 2618.

Lu, H.-Z., Liu,Y., Wang, C., Xu, Y., and Li, H., 2003. Mineralization and Fluid Inclusion study of the Shizhuyuan W-Sn-Bi-Mo-F Skarn deposit, Hunan Province, China. Economic Geology, 98, 955-974.

Makin, S.A., Simandl, G.J., and Marshall, D., 2014. Fluorite and its potential as an indicator mineral for carbonatite-related rare earth element deposits. In: Geological Fieldwork 2013, British Columbia Ministry of Energy and Mines, British Columbia Geological Survey Paper 2014-1, 207-212.

Mao, M., Simandl, G.J., Spence, J., and Marshall, D., 2015. Fluorite trace element chemistry and its potential as an indicator mineral: Evaluation of LA-ICP-MS method. In: Simandl, G.J. and Neetz, M., (Eds.), Symposium on Strategic and Critical Materials Proceedings, November 13-14, 2015, Victoria, British Columbia. British Columbia Ministry of Energy and Mines, British Columbia Geological Survey Paper 2015-3, pp. 251-264.

Mauthner, M. and Melanson, F., 2006. Fluorite occurrences in Canada. Rocks & Minerals, 81, 114-120.

McCammon, J.W., 1955. Rexspar Uranium and Metals mining Co. Limited. Minister of Mines, B.C., Annual report, 1954, pp. 108-111.

McLennan, S.M., 1994. Rare earth element geochemistry and the

"tetrad" effect. Geochimica et Cosmochimica Acta, 58, 2025-2033.
Min, M., Fang, C., and Fayek, M., 2005. Petrography and genetic history of coffinite and uraninite from the Liueryiqi granite-hosted uranium deposit, SE China. Ore Geology Reviews, 26, 187-197.
Misra, K.C. and Lu, C., 1992. Hydrothermal calcites from the Mississippi Valley-type Elmwood-Gordonsville zinc deposits, Central Tennessee, U.S.A.: Fluid inclusion and stable isotope data. European Journal of Mineralogy, 4, 977-988.
Monecke, T., Kempe, U., Monecke, J., Sala, M., and Wolf, D., 2002. Tetrad effect in rare earth element distribution patterns: A method of quantification with application to rock and mineral samples from granite-related rare metal deposits. Geochimica et Cosmochimica Acta, 66, 1185-1196.
Mortensen, J.K., Montgomery, J.R. and Fillipone, J., 1987. U-Pb zircon, monazite, and sphene ages for granitic orthogneiss of the Barkerville Terrane, east-central British Columbia. Canadian Journal of Earth Sciences, 24, 1261–1266.
Möller, P., Holzbecher, E., 1998. Eu anomalies in hydrothermal fluids and minerals. A combined thermochemical and dynamic phenomenon. Freiberger Forschungshefte, 475, 73– 84.
Möller, P., Parekh, P.P., and Schneider, H.-J., 1976. The application of Tb/Ca-Tb/La abundance ratios to problems of fluorspar genesis. Mineralium Deposita, 11, 111-116.
Pelch, M.A., Appold, M.S., Emsbo, P., and Bodnar, R.J., 2015. Constraints from fluid inclusion compositions on the origin of Mississippi Valley-Type mineralization in the Illinois-Kentucky district. Economic Geology, 110, 787-808.
Pell, J., 1992. Fluorspar and fluorine in British Columbia. British Columbia Geological Survey, Open file 1992-16.
Pell, J. and Hora, Z.D., 1987. Geology of the Rock Canyon Creek fluorite/rare earth element showing southern Rocky Mountains. In: Geological Fieldwork 1986, British Columbia Ministry of Energy and Mines, British Columbia Geological Survey Paper 1987-1, pp. 255-258.
Preto, V.A., 1978. Rexspar Uranium Deposit (82M/12W), B.C.. Ministry of Energy and Mines, Geological Fieldwork 1977, Paper 1978-1, 19-22.
Richardson, C.K. and Pinckney, D.M., 1984. The chemical and thermal evolution of the fluids in the Cave-in-Rock fluorspar district, Illinois: Mineralogy, paragenesis and fluid inclusions. Economic Geology, 79, 1833-1856.
Samson, I.M., Kerr, I.D., and Graf, C., 2001. The Rock Canyon Creek fluorite-REE deposit, British Columbia. In: Industrial Minerals in Canada. Canadian Institute of Mining, Metallurgy and Petroleum, Special Volume 53, 1-10.
Salvi, S. and Williams-Jones, A.E., 2006. Alteration, HFSE mineralization and hydrocarbon formation in peralkaline igneous systems: Insights from Strange Lake Pluton, Canada. Lithos, 90, 19-24.
Schofield, S.J., 1920. Geology and ore deposit of Ainsworth Mining Camp, British Columbia. Geological Survey of Canada, Memoir 117, 73p.
Schwinn, G. and Markl, G., 2005. REE systematics in hydrothermal fluorite. Chemical Geology, 216, 225-248.
Simandl, G.J., 2009. World fluorspar resources, market and deposit examples from British Columbia, Canada. British Columbia Geological Survey, Information Circular, 2009-4, 16p.
Staebler, G., Deville, J., Verbeek, E., Richards, R.P., and Cesbron, F., 2006. Fluorite: From ancient treasures to modern labs and collections. In: Fisher, J., Jarnot, M., Neumeier, G., Pasto, A., Staebler, G., and Wilson, T. (Eds.), Fluorite - the collector's choice. Lithographie, LLC, Connecticut, U.S.A. pp. 4-12.
Sylvester, P., 2008. Matrix effects in LA-ICP-MS. In: Sylvester, P. (Ed.), Laser Ablation–ICP–MS in the Earth Sciences current practices and outstanding issues. Mineralogical Association of Canada Short Course 40, Vancouver, B.C., pp. 67-79.
Taylor, S.R. and McLennan, S. M., 1985. The continental crust: its composition and evolution. Blackwell scientific publications, Oxford, 312p.
Trofanenko, J., Williams-Jones, A.E., and Simandl, G.J., 2014. The nature and origin of the carbonatite-hosted Wicheeda Lake rare earth element deposit. In: Geological Fieldwork 2013, British Columbia Ministry of Energy and Mines, British Columbia Geological Survey Paper 2014-1, pp. 213-225.
Verbeek, E., 2006. Fluorite Luminescence. In: Fisher, J., Jarnot, M., Neumeier, G., Pasto, A., Staebler, G., and Wilson, T. (Eds.), Fluorite - the collector's choice. Lithographie, LLC, Connecticut, U.S.A., pp. 13-19.
Whitney, D.L. and Evans, B.W., 2010. Abbreviations for names of rock-forming minerals. American Mineralogist, 95, 185-187.
Woodcock, J.R., 1972. Geology - Liard Fluospar Project, Mineral Claims TEE, TAM, FIRE, WEST, GEM, Liard Mining Division. British Columbia Ministry of Energy Mines and Petroleum Resources, Assessment report, No. 3975, 61p.
Wright, W.R., Mariano, A.N. and Hagni, R.G., 1998. Pyrochlore, mineralization, and glimmerite formation in the Eldor (Lake LeMoyne) carbonatite complex, Labrador Trough, Quebec, Canada. In: Proceedings of the 33rd Forum on the Geology of Industrial Minerals. Canadian Institute of Mining, Metallurgy and Petroleum; Special Volume, 50, pp. 205-213.
Xu, C., Taylor, R.N., Li, W., Kynicky, J., Chakhmouradian, A.R., and Song, W., 2012. Comparison of fluorite geochemistry from REE deposits in the Panxi region and Bayan Obo, China. Journal of Asian Earth Sciences, 57, 76-89.
Xu, C., Zhang, H., Huang, Z., Liu, C., Qi, L., Li, W., and Guan, T., 2004. Genesis of the carbonatite-syenite complex and REE deposit at Maoniuping, Sichuan Province, China: Evidence from Pb isotope geochemistry. Geochemical Journal, 38, 67-76.